Cross kit reconfiguration algorithm for enhanced output power of PV array during shading mismatch conditions

Mohd Faisal Jalil [a,*], Dushyant Sharma [a], R.C. Bansal [b,c,**]

[a] Department of Electrical Engineering, Aligarh Muslim University, Aligarh, India
[b] Department of Electrical Engineering, University of Sharjah, Sharjah, United Arab Emirates
[c] Department of Electrical, Electronic and Computer Engineering, University of Pretoria, Pretoria, South Africa

ARTICLE INFO

Keywords:
PV array reconfigurations
Odd-Even reconfiguration
TCT
Shade dispersion
Mismatch losses

ABSTRACT

Maintaining the uniform irradiance in an extensive photovoltaic (PV) system is almost impossible. The mismatch between panels of a PV array results in substantial power loss. The PV panels in an array are reconfigured by the proposed Cross-Kit (CK) technique to obtain optimal power output for different partial shade situations (PSS). The suggested approach allows the structure to balance the shade effect across the entire PV array with different physical places of panels. The PV modules are linked using the Total Cross Tied (TCT) configuration, and the CK technique decides the physical placement of modules within the array. The electrical connections of the TCT-linked PV array are unaffected by the CK panel configurations. The PV array's output arranged with the suggested CK method is assessed and contrasted with TCT and Odd-Even (OE) reconfiguration for mathematical and experimental validation. Four different PSS are taken into consideration. The percentage instantaneous maximum power improvement compared to TCT and OE ranges from 5.49% to 26.73%. The benefits of the suggested approach include straightforward guidelines for implementation, explanation of the P-V plots, and a reduced charge of maximum power point tracking.

1. Introduction

Renewable energy sources (RES) have gained popularity in recent years and have mostly replacing other conventional sources of energy. The Geothermal, biomass, wind, and solar energy sources are a few forms of RES. Due to its prevalence and accessibility in nature, solar power is the most necessary and basic sustainable energy resource among all others [1,2]. Sustainable development is made possible by the infinite supply and clean production of electricity provided by solar photovoltaic panels. In addition to requiring little servicing, the energy generated by photovoltaic (PV) system is almost pollution- and fuel-free. Additionally, PV energy is used in a variety of settings, including rural areas, street lighting, residential structures, and power system engineering. Partial shadings are one of the most significant difficulties that have a considerable impact on PV module efficiency. Partial shadowing happens when the PV modules in the array are shadowed by flying birds, moving clouds, nearby buildings, etc. When PSCs are present, the shaded module receives less irradiance than the non-shaded modules. Because shaded PV modules restrict an array's current output, mismatch losses affect the overall PV system and may harm the PV modules or cells [3,4]. Bypass diodes can be connected across the terminals as one

* Corresponding author.
** Corresponding author at: Department of Electrical Engineering, University of Sharjah, Sharjah, United Arab Emirates.
E-mail addresses: mfaisaljalil@gmail.com (M.F. Jalil), rcbansal@ieee.org (R.C. Bansal).

Nomenclature

BL	Bridge link.
BIPV	Building integrated PV.
CK	CROSS-KIT method.
CVT	Constant voltage tracking.
DB	Dwarf Board.
DBSS	Dwarf Board Shading Situation.
DE	Differential evolution.
DN	Dwarf Narrow.
DNSS	Dwarf Narrow Shading Situation.
DSO	Digital storage oscilloscope.
ER	Execution Ratio.
FF	Fill-factor.
EAR	Electrical Array Reconfiguration.
GMPP	Global maximum power point.
GP	Global peak.
HC	Honey-comb.
I-V plots	Current Voltage characteristics.
LMPP	Local maximum power point.
ML	Mismatch losses.
MPPT	Maximum power point tracking.
OE	ODD-EVEN method.
OVT	Open-circuit voltage tracking.
P-V plots	Power voltage characteristics.
PAC	Photovoltaic array configuration.
PSCs	Partial shading conditions.
PVR	Photovoltaic array reconfiguration.
PSO	Particle swarm optimization.
PV	Photovoltaic.
RES	Renewable energy sources.
SP	Series parallel.
SS	Simple series.
TB	Tall Board.
TBSS	Tall Board Shading Situation.
TCT	Total cross tied.
TN	Tall narrow.
TNSS	Tall narrow Shading Situation.

method of guarding against harm to the darkened PV modules. The PV array's P-V and I-V curves exhibit several steps and various peaks after the installation of bypass diodes [5]. One global peak (GP), also known as the global maximum power point (GMPP) [6]. It is the single peak among the many that provides the greatest maximum power. While all other local optimum power points are smaller (LMPPs). The presence of the array configuration, the way the modules are shaded, and where they are physically placed inside the PV array all have an impact on the sum of power produced. Because there's a partial shade numerous peaks can start causing the maximum power point tracking (MPPT) method to operate at the low-optimum power points (LMPPs) instead of the high-maximum power point (GMPP), which wastes more power [7,8].

To the contrary, the maximum power output is severely impacted through the PV array arrangement. Consequently, in PSCs, it's important to choose the appropriate configuration. For example, "Total cross tied (TCT), honeycomb (HC), bridge-link (BL), series-parallel (SP), simple-series (S) and parallel (P)," are some of the PV array configurations. Many researchers have focused on keeping mismatch losses from slight shadows to a minimum [9,10]. Mismatch loss raises overall losses instigated by small differences in the electrical properties of the modules, which are expressed as a set percentage lessening in the system's DC output power. The authors in [11], examined three PV array designs, including TCT, BL, and SP, a probability - based framework is employed to evaluate consistency during mismatch problems induced by fabrication tolerance. According to this study, TCT and BL PV array topologies are more reliable and reduce mismatch losses than SP PV arrays. A study and evaluation of various PV array topologies, including "SS, SP, TCT, BL, and HC" under different partial shade conditions, are provided different studies [12,13]. The researchers used a variation of metrics to assess each configuration's performance throughout the investigation. The observed result demonstrates that, in comparison to alternative configurations, the TCT PV array minimize mismatch losses [14]. In this study, performance parameter are, the GMPP, ML, FF, and array efficiency. Compared to alternative PV array topologies, this research guarantees that the TCT PV array increases the optimum global power. However, a significant drawback of the TCT design is that it limits the output current of an array, if many PV

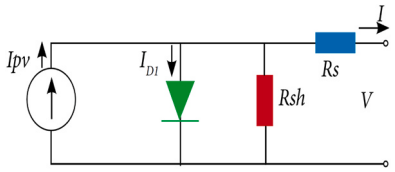

Fig. 1. Corresponding circuit of Photovoltaic cell for one diode model.

Table 1
Specifications of PV module (1000 W/m^2, 25°C).

Systems parameters	Values under optimal operational circumstances
Maximum output power	200.143 W
Max. power current	7.61 A
Short circuit current	8.21 A
Max. power voltage	26.3 V
Open circuit voltage	32.9 V
No. of cells linked in series	54

modules are darkened in a row [15,16]. To solve this problem, many researchers have suggested TCT array reconfiguration strategies that steadily transfer the shading effects of one row on the rows next to it and reducing mismatch losses under PSCs [17,18].

The reconfiguration procedures are categorized as dynamic and static methods. Static reconfiguration techniques change the physical arrangement of PV panels in certain locations to spread partial shading outcomes across the array. These do not dynamically change the panel's placement. Specifically, regardless of the shading situation, the module's physical location is fixed[19]. Dynamic reconfiguration approaches alter the electrical connections of the PV modules while leaving their actual locations unaltered. Techniques for static reconfiguration do not require a large number of sensors and switches. Under different irradiance levels, however, the connectivity structure remains constant. For static approaches to work, skilled individuals must make physical changes to the PV panel. As a consequence, there is a limited scope for static reconfiguration approaches in small-scale PV array architectures[20]. The static reconfiguration techniques are one-time PV panel placement in the array that occasionally make use of shade dispersion techniques based on puzzles, circular shift techniques, rule-based mathematical techniques, and engineering approach-based techniques[21–23].

Additionally, a number of dynamic reconfiguration strategies have been explored in the past to mitigate the effects of mismatch condition. Dynamic reconfiguration's simple concept is that, in the event of partial shadowing, altering the contacts of the solar PV sub-modules with a switching matrix can immediately reduce mismatch loss. The system may switch between parallel and series connections with the use of a switching matrix[24]. However, the discretion of an adequate PV array connector, which can reduce shading effects, has signaled the start of the real dynamic reconfiguration [25]. Some of them use adaptive array reconfiguration technique [26], equalization index (EI) [27], and adaptive reconfiguration procedure [28]-based optimization algorithms. The PV plant and the inverter can be connected with various modules using a variable connection scheme (VCS). The branch and bound method is used to resolve the mixed-Integer quadratic programming (MIQP) method [29]. A hierarchical and iterative categorization method based on the idea of insolation equalization is used to get the optimal configuration. It involves complicated control procedures and more hardware than a static PV array [30]. The entire solar array is classified into two halves, a male and a female, in the couple matching best generation algorithm. There are exactly as many rows and nearly as many columns in each segment [31]. In partially shadowed environments, the power comparison technique (PCT) was created to maximize PV array power output [32], and practically all current reconfiguration techniques apply the irradiance equalization concept. The insolation equalization concept helps to improve the output power of a solar array. Because of this, algorithms for reconfiguring systems based on this idea sometimes fail to achieve the global optimum configuration [33,34]. In every ecological situation, an array reconfiguration scanning technique was reported to optimize the array's available power [35,36]. However, in order to implement the method, it requires sensors and a switching structure circuit. To modify the interconnections of PV modules and lessen mismatch losses, Fuzzy logic estimators were used to come up with a plan for self-adaptive reconfiguration. The fuzzy algorithm reacts rapidly to changes in the outer environment. However, in order to reconfigure the array and reduce losses, all of the previous re-configuration techniques require switches and sensors. The addition of such switches and sensors raises the expense of the PV array and increases the difficulty of the needed software and hardware.

Static reconfigurations is combatively less complex, reliable and cost effective. Since for all shading states, the positioning of the module is fixed, they do not dynamically change it. In the literature, an optimum TCT design that takes into account sunlight levels, shading situations, and the duration of each shadow position was presented as a way to reduce mismatch loss through mathematical formulation [37]. However, it is difficult to enhance such a system since calculations must be made based on the shading data, especially for uneven shading situations in large arrays. The authors in [38] described how modules coupled in a TCT layout were physically assembled once. Without altering their electrical connections, the modules are physically placed in accordance with the Sudoku puzzle's grid to accommodate different insolation environments [19]. As the Odd-Even (OE) reconfiguration technique is used to form the TCT configured array on the basis of OE sequence situation. This configuration disperses the effects of shade throughout the array, boosting PV power. It has been explained how a PV module would react to certain shadows. Additionally, a mathematical method has been developed to quantify the shadow impact in order to reduce mismatch loss caused by renumbering panel

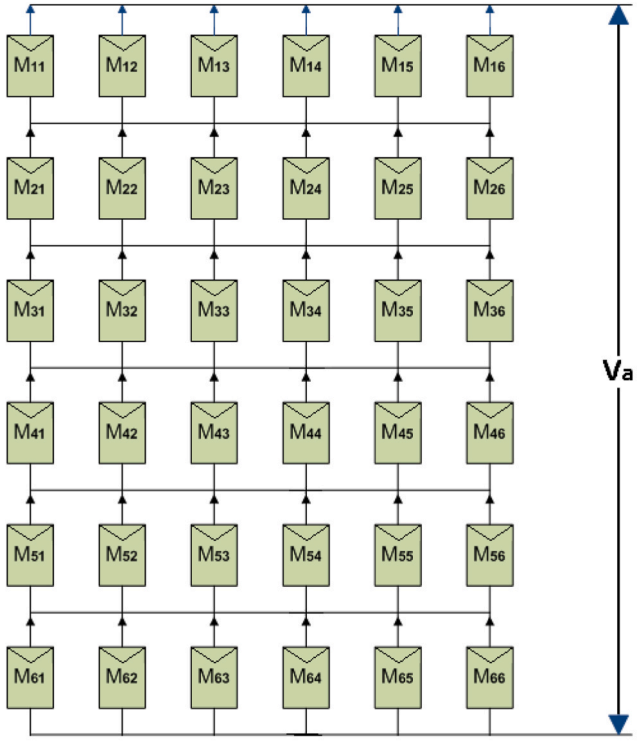

(a). TCT linked array.

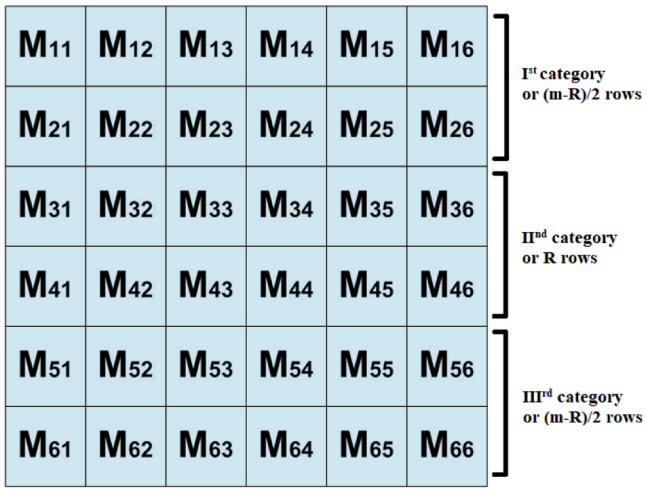

(b). TCT arrangement for an array of 6×6.

Fig. 2. (a). TCT linked array. (b). TCT arrangement for an array of 6 × 6.

arrangements under various shading situations [39]. The complex reconfiguration rules with limited application in terms of size and order of the PV array low shade dispersion in the most prominent shading conditions have been addressed with the proposed CK technique. The main objective of this investigation is to raise the economic feasibility, efficiency, and reliability of PV arrays to facilitate the broader adoption of PV power generation.

The CROSS-KIT technique (CK) is suggested to increase energy output further and streamline the topology layout for a PV array relying on the TCT configuration. In the proposed method, the modules' physical placement and circuitry layout in a TCT-layout PV array are changed according to the CK puzzle solutions to disperse the shade effect throughout the array. The CK is intended to reduce the PSC impact, mainly in most prominent shading conditions. The suggested CK geometry offers distinct benefits, such as easy rules, quick execution, and fewer LMPPs, which improve the P-V curves and, consequently, the MPPT work. The effectiveness of the

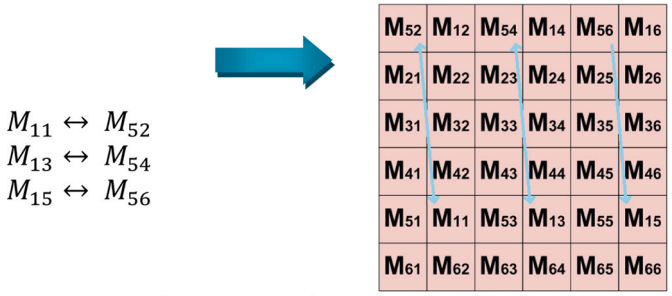

(a). Replacement of I[st] category modules according to rule 1.

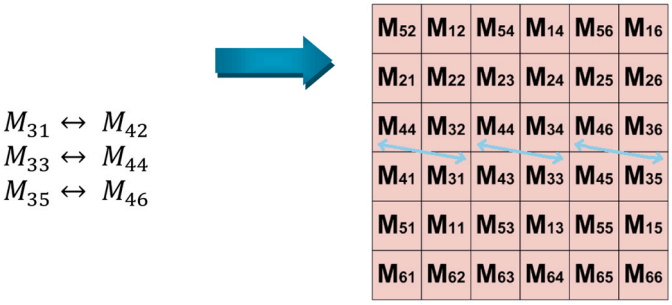

(b). Replacement of modules of II[nd] category according to Rule 2.

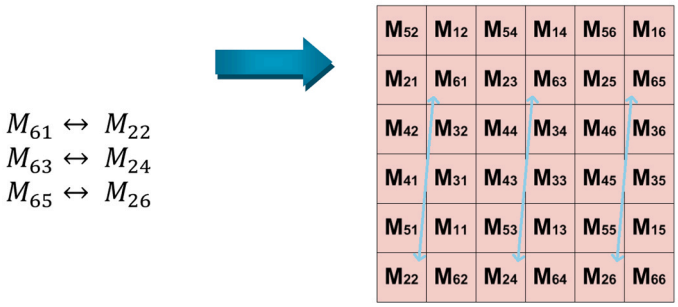

(c). Replacement of modules of III[rd] category according to Rule 3.

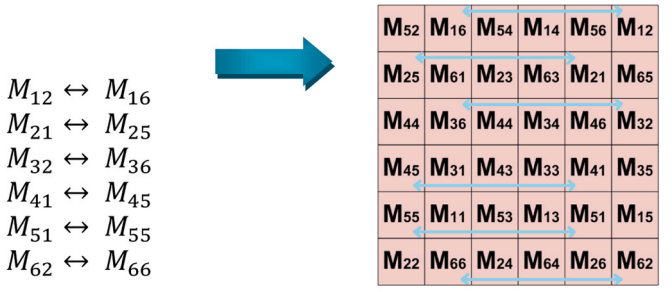

(d). Replacement of modules according to Rule 4.

Fig. 3. (a). Replacement of I[st] category modules according to rule 1. (b). Replacement of modules of II[nd] category according to Rule 2. (c). Replacement of modules of III[rd] category according to Rule 3. (d). Replacement of modules according to Rule 4. (e). Summarised CROSS-KIT method.

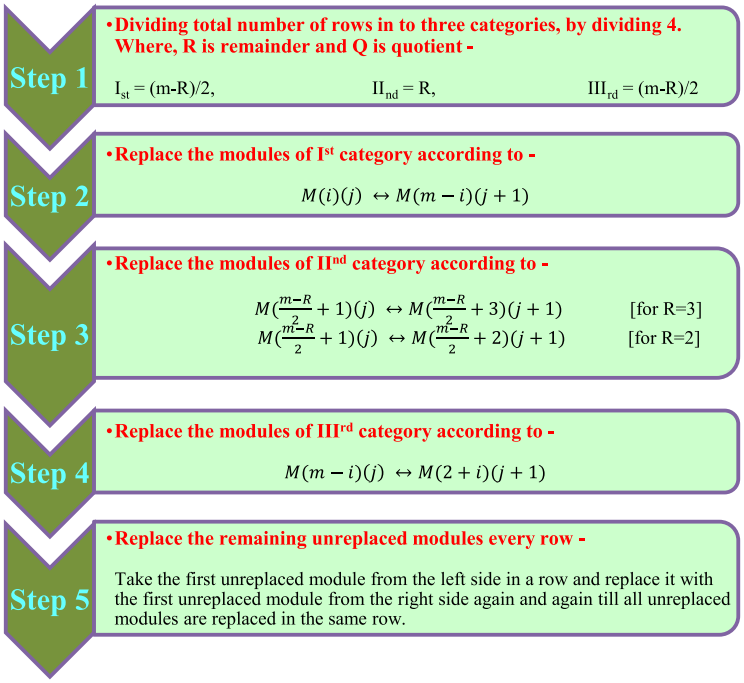

(e). Summarised CROSS-KIT method.

Fig. 3. (*continued*).

configuration technique presented in this study is also evaluated using four power-loss estimation indices for comparability: the shading losses, mismatch losses, percentage execution ratio and power improvement.

The suggested method demonstrates superiority in distributing shadow situations and boosting PV power output. The order of the remaining portions of the manuscript is as follows: A thorough explanation of the system under consideration is provided in Section 2. The proposed approach, which relies on Cross-Kit, is presented in Section 3. Section 4 includes validation and analysis. Sections 5, 6, and 7 compare the proposed technique with the TCT and Odd-Even algorithms. Experimental validation of Cross-Kit and comparative analysis is provided in Section 8. Lastly, Section 9 summarizes the key conclusions.

2. PV reconfiguration

The electrical properties of the solar panel must be understood in order to reconfigure a photovoltaic array. In earlier research studies, a number of PV cell representations have been existing. These are the one-diode models, two-diode, three-diode, and [40,41]. The type with a single diode is the one that is most often used. Fig. 1 shows the arrangement and features of one diode models. And output voltage and current are given by Eqs. (1–4). Because of its good accuracy and simplicity, the one-diode model is often used to illustrate the performance of PV modules [42,43].

Output I:

$$I_{D1} = I_{01}(e^{V_{D1}/\alpha_1 V_t} - 1) \tag{1}$$

$$I = I_{pv} - (I_{D1} + \frac{V_{D1}}{R_{sh}}) \tag{2}$$

Output V:

$$V = V_D - IR_S \tag{3}$$

$$V_t = N_S kT/q \tag{4}$$

Where, α = diode's ideality factor, T = PV Cell's temperature in Kelvin, q= electron's charge, and N_S = sum of cells in series. The characteristics of the PV module for consideration under standard working circumstances are listed in Table 1.

3. Cross-Kit configured structure for PV array

This paper describes a Cross-Kit method for the arrangement of PV array's module. The suggested PV array configuration approach

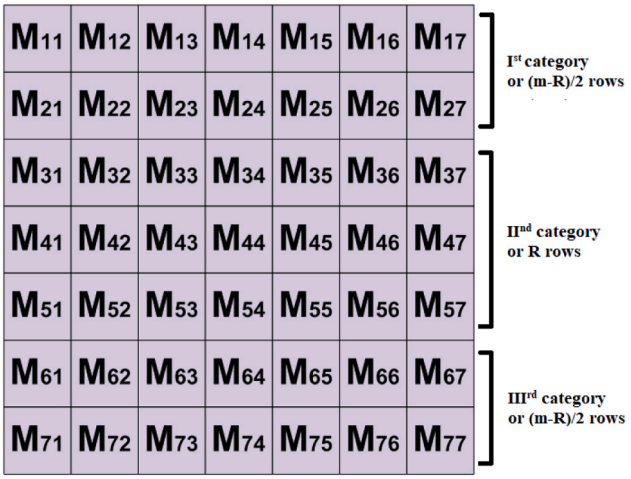

(a). TCT arrangement for a 7×8 ordered array.

(b). CROSS-KIT arrangement for a 7×8 ordered array.

Fig. 4. (a). TCT arrangement for a 7 × 8 ordered array. (b). CROSS-KIT arrangement for a 7 × 8 ordered array.

is categorized into two sections. The first section is about the scheme to connect the PV array's modules electrically. The suggested approach uses the same electrical connections as the TCT configuration. The second section is about the PV array's actual module configuration, as mentioned below. Consider the m×n order of the PV array with represents m rows and n columns, respectively. Each PV array panel is identified by the letters M_{ij}. Here i (i = 1,2,3,…m) and j (j = 1,2,3,.n) denote the row and column, correspondingly. Where the module is connected electrically. The TCT layout with PV array electrical connections is shown in Fig. 2(a). M_{24}, for instance, indicates that the module is linked to the PV array's second row and fourth column (see Fig. 2(b)).

In the suggested structuring approach, first the total rows of PV array are divided into three categories. These three categories are identified by dividing the total number of rows (m) by 4. By division we get R as remainder and Q as quotient. So, the three categories are:

I. (m-R)/2 rows are in the Ist category (counting from the first row, top to bottom),
II. R rows are in the IInd category (counting from the next row where the Ist category ended),
III. (m-R)/2 rows are in the IIIrd category (counting from the next row where the IInd category ended).

Categorizations of the rows should always start from top to bottom. Starting of next category should always starts from the next row after ending of previous category.

Example- According to Fig. 2(b), there are rows in all, totalling m = 6. The overall number of rows is divided by 4. Results in the reminder, R = 2. The three categories for the array presented in Fig. 2(b) are categorized from top to bottom (always) as follows:

- Ist category = number of rows is 2 (in the top-most section, rows 1 and 2).
- IInd category = number of rows is 2 (in the middle section, rows 3 and 4).

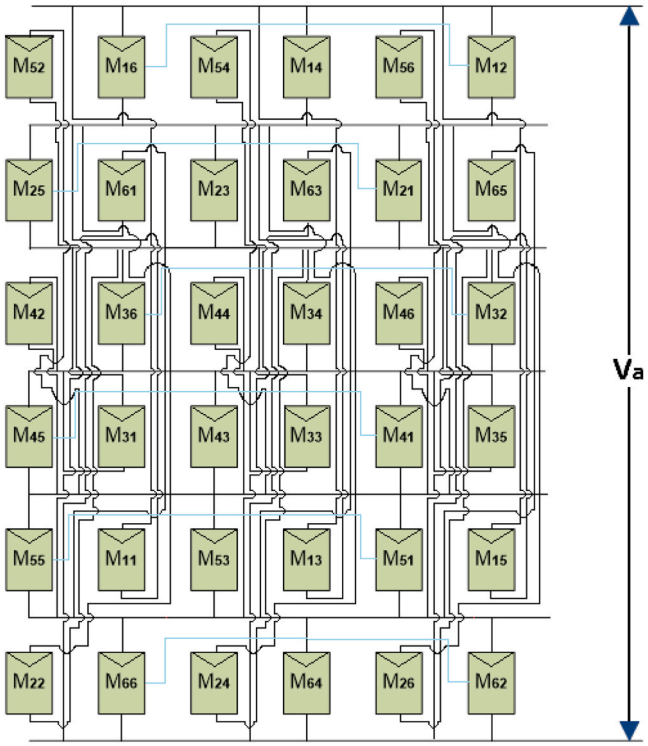

(a). CROSS-KIT structure of an array.

M52	M16	M54	M14	M56	M12
M25	M61	M23	M63	M21	M65
M44	M36	M44	M34	M46	M32
M45	M31	M43	M33	M41	M35
M55	M11	M53	M13	M51	M15
M22	M66	M24	M64	M26	M62

(b). TCT arrangement for an array of 6×6.

Fig. 5. (a). CROSS-KIT structure of an array. (b). TCT arrangement for an array of 6 × 6.

- IIIrd category = number of rows is 2 (in the bottom section, rows 5 and 6).

After the categorization of the total number of rows, there are a total of four rules, as given below, to reconfigure the modules of any order of array.

Rule-1: Replace the modules of Ist category according to Eq. (5):

$$M_{ij} \leftrightarrow M_{(m-i)(j+1)} \tag{5}$$

Module of i^{th} row and j^{th} column replace with module of $(m-i)^{th}$row and $(j+1)^{th}$column. Where, $i = 1,3,5,7\ldots$m (odd number) and $j = 1,3,5,7\ldots$n (odd number). The PV array's m and n variables stand for the total number of rows and columns, respectively.

Example- Rendering to the Ist category categorization to the array displayed in Fig. 2(b), $i = 1$, and $j = 1,3$, and 5. The collection of modules that are to be replaced according to rule 1 are M_{11},M_{13},and M_{15} (all possible combinations of given i and j for the Ist category as 11, 13, and 15). As a result of rule 1 (Eq. 5), the modules of the Ist category will be replaced as shown in Fig. 3(a):

Rule-2: Replace the modules of IInd category according to Eqs. (6 and 7):

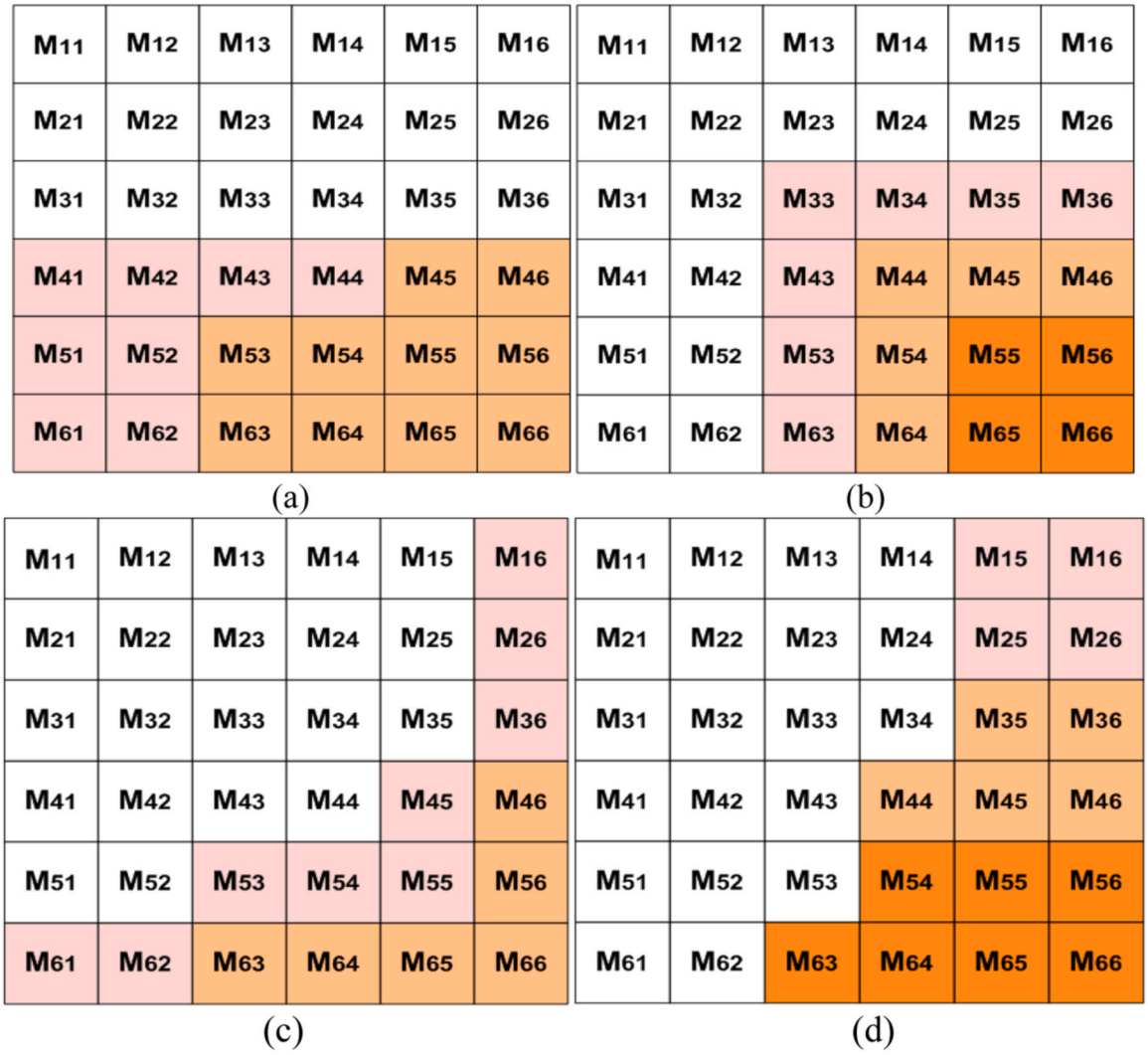

Fig. 6. (a-d). Four different types of shading situations exist: (a) DB, (b) TB, (c) DN, and (d) TN.

$$(a) M_{\left(\frac{m-R}{2}+1\right)\left(j\right)} \leftrightarrow M_{\left(\frac{m-R}{2}+3\right)\left(j+1\right)}, (\text{if R} = 3) \tag{6}$$

$$(b) M_{\left(\frac{m-R}{2}+1\right)\left(j\right)} \leftrightarrow M_{\left(\frac{m-R}{2}+2\right)\left(j+1\right)}, (\text{if R} = 2) \tag{7}$$

- If R = 3, module of $\left(\frac{m-R}{2}+1\right)^{th}$ row and j^{th} column, replace with a module of $\left(\frac{m-R}{2}+3\right)^{th}$ row and $(j+1)^{th}$ column. Where $i = \frac{m-R}{2}+1$ and j = 1,3,5,7…n (odd number).
- if R = 2, module of $\left(\frac{m-R}{2}+1\right)^{th}$ row and j^{th} column, replace with a module of $\left(\frac{m-R}{2}+2\right)^{th}$ row and $(j+1)^{th}$ column. Where $i = \frac{m-R}{2}+1$ and j = 1,3,5,7…n (odd number).
- If R= 1, then skip this row (the middle row) as it is till the execution of rule 3. After then, replace the modules of this row according to rule 4.

Example- According to the IInd category categorization for the array depicted in Fig. 2(b), $i = 3$, and j = 1,3, and 5. The collection of modules that are to be replaced according to rule 2 are M_{31},M_{33},and M_{35} (all possible combinations of given i and j for the IInd category as 31, 33, and 35). As a result of rule 2 (Eq. 7, because R = 2), the modules of the IInd category will be replaced as shown in Fig. 3(b):

Rule-3: Replace the modules of IIIrd category according to Eq. (8):

Table 2
Parameters of conventional configurations in all four considered shading state.

	P_{max} (W)	V_{max} (V)	V_{oc} (V)	I_{sc} (A)
Shading State 1 (SS1)				
TCT	3993	168.5	193.7	49.24
SP	3904	166.6	193.6	49.24
BL	3925	167.4	193.7	49.24
HC	3923	167.3	193.7	49.24
Shading State 2 (SS2)				
TCT	4346	166.5	194.0	49.23
SP	4034	160.6	193.4	49.24
BL	4063	160.8	193.4	49.23
HC	4081	161.0	193.5	49.23
Shading State 3 (SS3)				
TCT	4919	137.0	194.8	46.7
SP	4713	136.8	194.8	46.79
BL	4813	136.8	194.8	46.78
HC	4786	136.4	194.8	46.79
Shading State 4 (SS4)				
TCT	3699	140.0	193.0	44.3
SP	3760	115.0	192.1	44.32
BL	3558	137.2	192.7	44.32
HC	3674	140.9	192.4	44.31

$$M_{(m-i)(j)} \leftrightarrow M_{(2+i)(j+1)} \tag{8}$$

Module of row $(m-i)^{th}$ and j^{th} column replace with module of $(2+i)^{th}$ row and $(j+1)^{th}$ column) Where, $i = 0,2,4,6\ldots$m (even number include 0) and $j = 1,3,5,7\ldots$n (odd number).

Example- According to the III[rd] category categorization for the array depicted in Fig. 2(b), $i = 3$, and $j = 1,3$, and 5. The collection of modules that are to be replaced according to rule 3 are $M_{61}, M_{63},$ and M_{65} (all possible combinations of given i and j for the IIIrd category as 61, 63, and 65). As a result of rule 3 (Eq. 8), the modules of the IIIrd category will be replaced as shown in Fig. 3(c):

Rule 4: Replace the remaining not replaced modules according to the following statement:

Take the first not replaced module from the left side in a row and replace it with the first not replaced module from the right side. Follow this operation for the same row again and again till all not replaced modules are replaced in the same row. And apply the same operation for every row from top to bottom, if possible (any two not replaced module is exist in a row).

Example. After applying rules 1, 2, and 3 in Fig. 2(b), the not replaced modules in each row are $M_{12}, M_{14}, M_{16}, M_{21}, M_{23}, M_{25}, M_{32}, M_{34}, M_{36}, M_{41}, M_{43}, M_{45}, M_{51}, M_{53}, M_{55}, M_{62}, M_{64},$ and M_{66}. As a result of rule 4, the unreplaced modules in each row will be replaced as follows:

If, in any row, a single not replaced module is remaining after applying rule 4, like $M_{14}, M_{23}, M_{34}, M_{43}, M_{53},$ and M_{64}. So, skip these modules as they are and apply rule 4 for the next row.

Hence, after the implementation of all four rules as mentioned above, Fig. 5(b) shows the final CROSS-KIT reconfigure arrangement for an array of the order of 6 × 6. To further understand this technique, let's use a new example of order 7 × 8 shown in Fig. 4(a) with all above simple steps of CROSS-KIT method summarised in Fig. 3(e). For the order of 7 × 8 TCT configuration category, CROSS-KIT structuring is displayed in Fig. 4(b).

4. System of modules for investigation

The investigation will focus on an array of size 6 × 6 with a CROSS-KIT structure. Fig. 5(b) illustrates the structure. For this TCT-linked PV array, the CROSS-KIT design is created following the approach stated in Section 3. Figs. 2(a) and 5(a) show that the electrical composition of PV arrays stays unchanged while the actual placement of PV panels changes. As there is no change in the electric arrangement, the I-V relationships in the CROSS-KIT configuration are the same as for the TCT structure. This configuration reduces panel bypassing and improves the spreading of shade effects over the whole PV array. As a result, the output power will be enhanced for several shading designs.

5. Shading conditions and conventional configurations

The following shading state studies have been realized for use in this study's investigation using various shading effects. However, as previously mentioned, each Shading state is positioned in a CROSS-KIT array of order 6 × 6.

- Shading state I: Dwarf Broad Shading Situation (DBSS)
  In this shading situation, Shaded areas are present in all of the columns and a few rows, as shown in Fig. 6(a).
- Shading state II: Tall Broad Shading Situation (TBSS)
  In this shading situation, Shaded areas are present in the few columns and a few rows, as shown in Fig. 6(b).

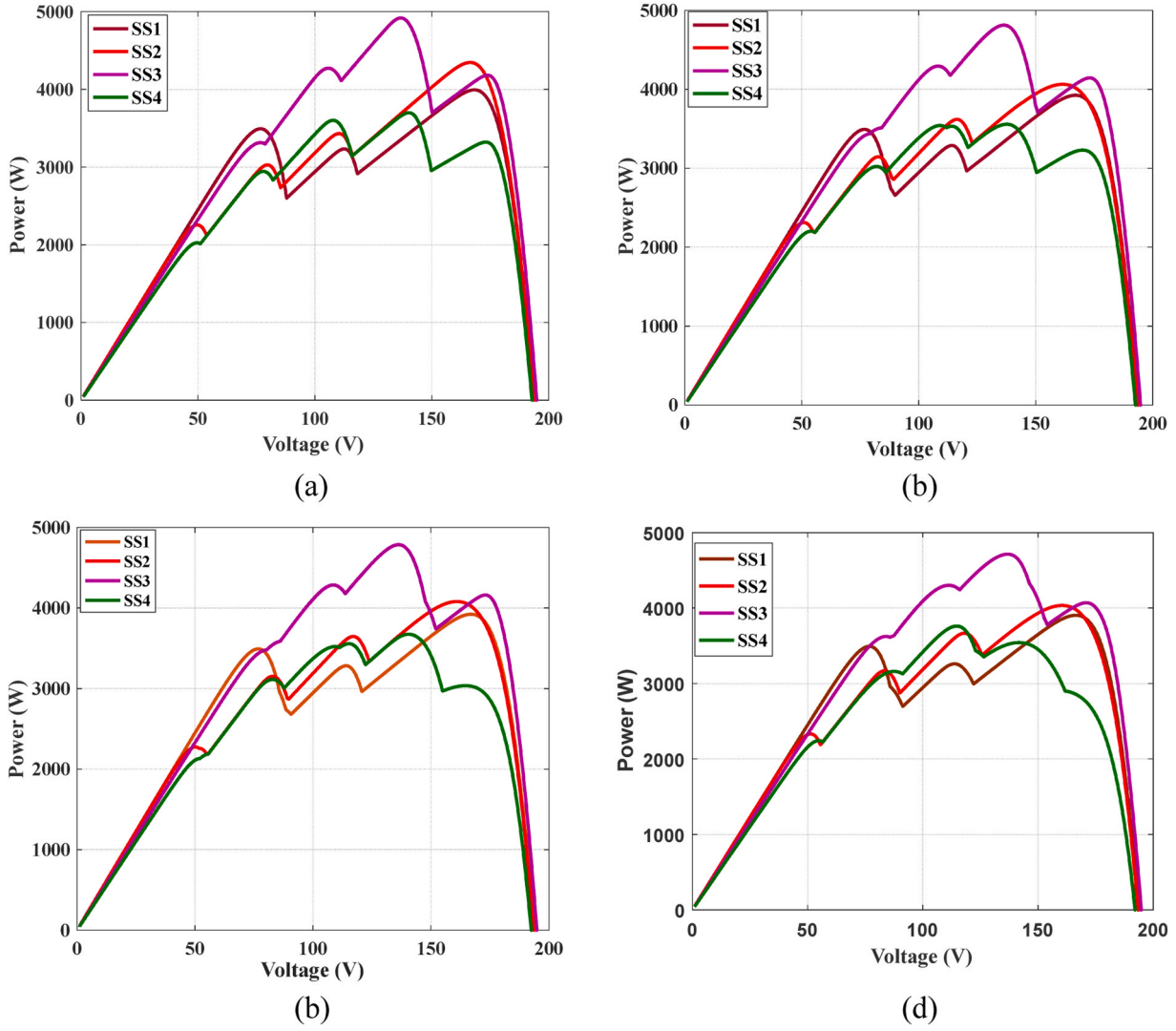

Fig. 7. (a-d): (a) P-V characteristics for TCT arrangement, (b) P-V characteristics for BL arrangement, (a) P-V characteristics for HC arrangement, and (b) P-V characteristics for SP arrangement.

- Shading state III: Dwarf Narrow Shading Situation (DNSS)
  In this shading situation, Shaded areas are present in all of the columns and all rows, as shown in Fig. 6(c).
- Shading state IV: Tall Narrow Shading Situation (TNSS)

In this shading situation, Shaded areas are present in all of the rows and a few columns., as referred in Fig. 6(a).

Different PV array connection strategies can be used under partial shade conditions to minimize the adverse effects of shading and maximize the overall energy generation. SP, TCT, BL, and HC are four frequently employed connection techniques.

PV modules are separated into strings connected in series, and subsequently connected in parallel in the series-parallel connection method. With this design, the system as a whole can produce more voltage and make greater use of the sunlight that is available. However, if only one module in a string is shaded, the performance of the entire string may suffer. The TCT connection approach addresses the SP technique's drawbacks. The modules are connected in a cross-tied configuration, and each module contains bypass diodes. By offering numerous parallel pathways for current flow, this configuration lessens the impact of shade on the entire system. The BL connection arrangement is comparable to the TCT scheme but uses more diodes to improve system performance. This approach lessens the effects of shading and enhances energy production by giving shaded modules extra bypass pathways. A honeycomb-like pattern is created by connecting PV modules using the HC connection scheme.

Among these techniques, TCT arrangement more effectively reduces the effect of partial shading on the PV array's output power, as presented in Table 2. The Power-Voltage curve for all considered shading states are shown for TCT, BL, HC, and SP arrangements, respectively, as represented in Fig. 7(a-d).

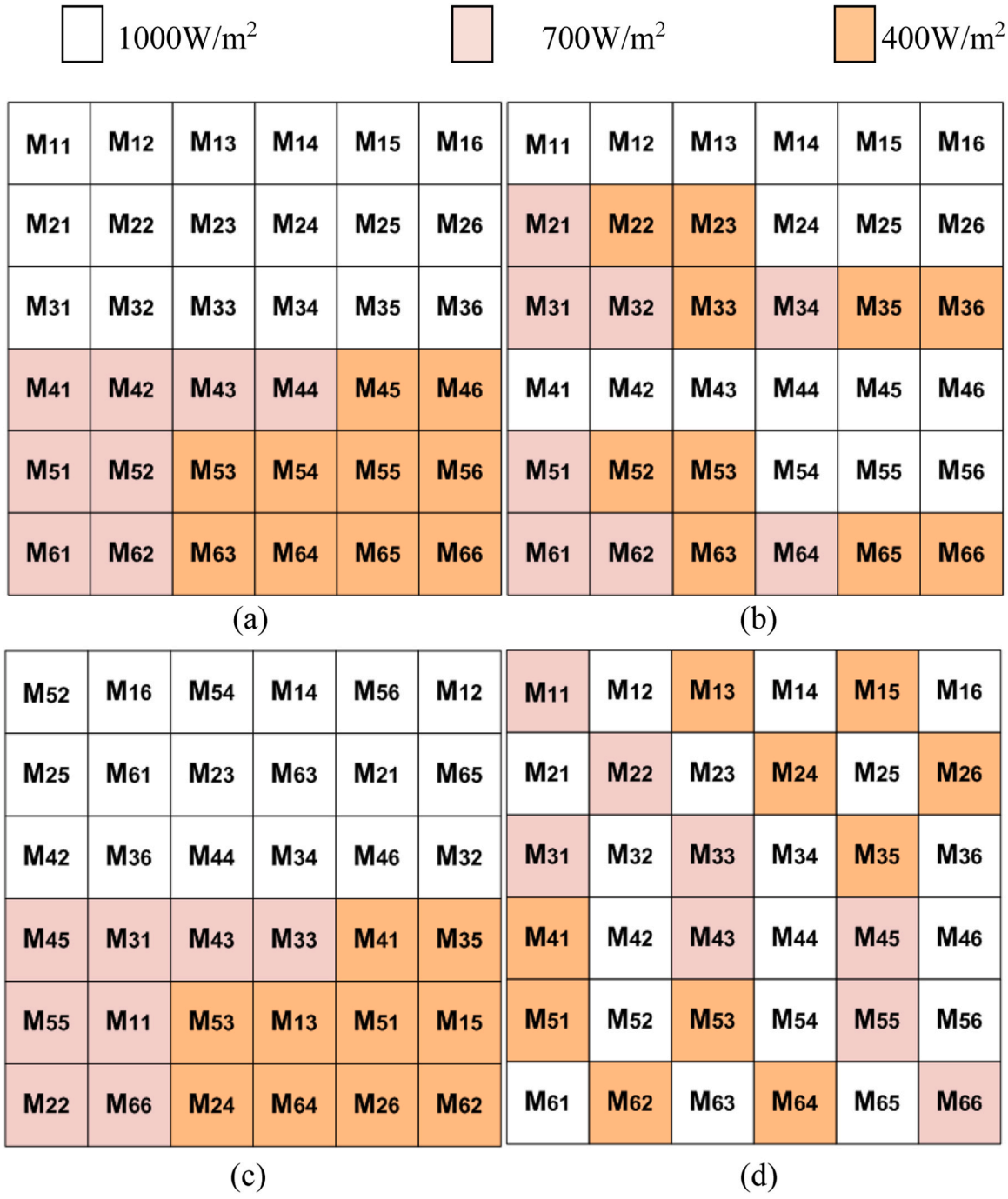

Fig. 8. (a-d): (a) DW shading situation for TCT arrangement, (b) DW shade distribution for ODD-EVEN configuration, (a) DW shading situation for CROSS-KIT configuration, and (b) DW shade dispersion for CROSS-KIT configuration.

6. Results and discussion

A 6 × 6 PV array connected in a TCT arrangement is subjected to four different shading scenarios in order to evaluate the efficacy of the suggested technique. The position of GP is theoretically calculated for the TCT, ODD-EVEN, and CROSS-KIT configurations. The position of GP shows how many rows are skipped in order to maximize the power. The theoretical findings are tested through simulation tests done in the MATLAB/Simulink system. For each shade situation, the TCT, ODD-EVEN, and CROSS-KIT arrangements are used to determine the PV parameters, and the outcomes are then presented.

Table 3
Spot of Global Peak in TCT, OE, and CROSS-KIT assemblies-Shading state I.

TCT arrangement				**Odd-Even arrangement**				**Cross-Kit arrangement**			
Row current with panels bypassed in the specified sequence		Voltage (V_a)	Power (P_a)	Row current with panels bypassed in the specified sequence		Voltage (V_a)	Power (P_a)	Row current with panels bypassed in the specified sequence		Voltage (V_a)	Power (P_a)
I_{R6}	3.0 I_m	6 V_m	18.0 V_m I_m	I_{R6}	3.3 I_m	6 V_m	19.8 V_m I_m	I_{R6}	4.5 I_m	6 V_m	27.0 V_m I_m
I_{R5}	3.0 I_m	-	-	I_{R3}	3.3 I_m	-	-	I_{R5}	4.5 I_m	-	-
I_{R4}	3.6 I_m	4 V_m	14.4 V_m I_m	I_{R5}	4.5 I_m	4 V_m	18.0 V_m I_m	I_{R2}	4.5 I_m	-	-
I_{R3}	6.0 I_m	3 V_m	18.0 V_m I_m	I_{R2}	4.5 I_m	-	-	I_{R1}	4.5 I_m	-	-
I_{R2}	6.0 I_m	-	-	I_{R4}	6.0 I_m	2 V_m	12.0 V_m I_m	I_{R4}	4.8 I_m	2 V_m	9.6 V_m I_m
I_{R1}	6.0 I_m	-	-	I_{R1}	6.0 I_m	-	-	I_{R3}	4.8 I_m	-	-

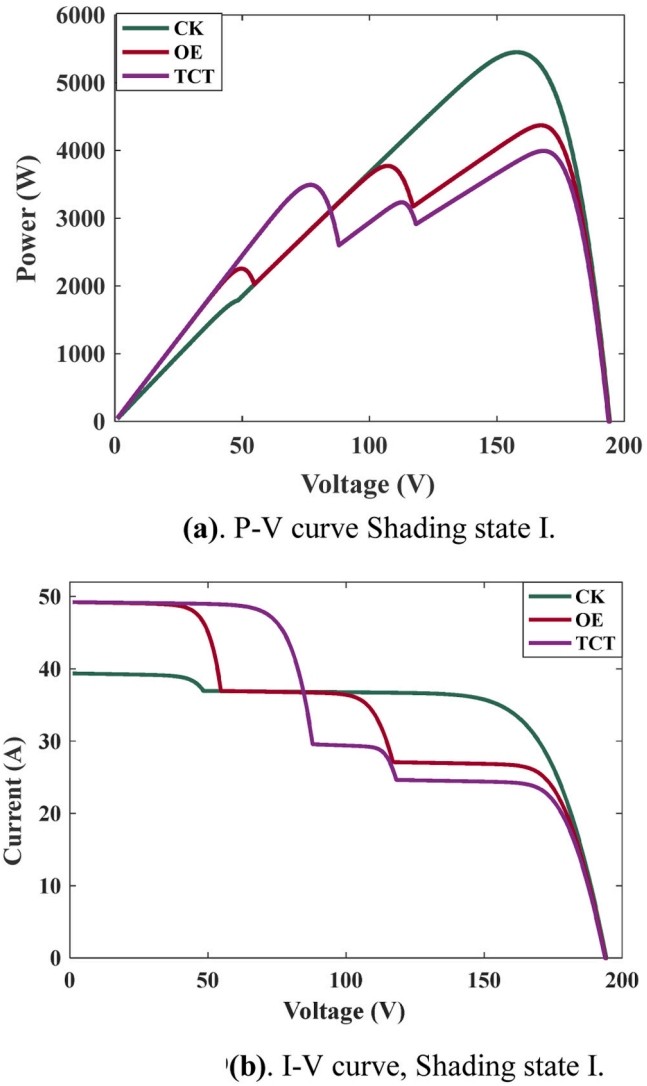

Fig. 9. (a). P-V curve Shading state I. (b). I-V curve, Shading state I.

The proposed Cross Kit reconfiguration technique mitigates the effects of partial shading conditions using a one-time arrangement to reconfigure the panels. In contrast, the dynamic reconfiguration technique changes module connections per the shading conditions and, therefore, can be more effective in shade dispersion with higher cost, complexities, sensors and switches. The proposed Cross Kit (CK) Reconfiguration technique has an efficient PV array design, reducing implementation complexities without adding extra cost to the system. The CK design will focus on lowering mismatch losses under practical operating conditions. The strategy reduces the likelihood of several local maxima, reducing the requirement for a complicated maximum power point tracking algorithm.

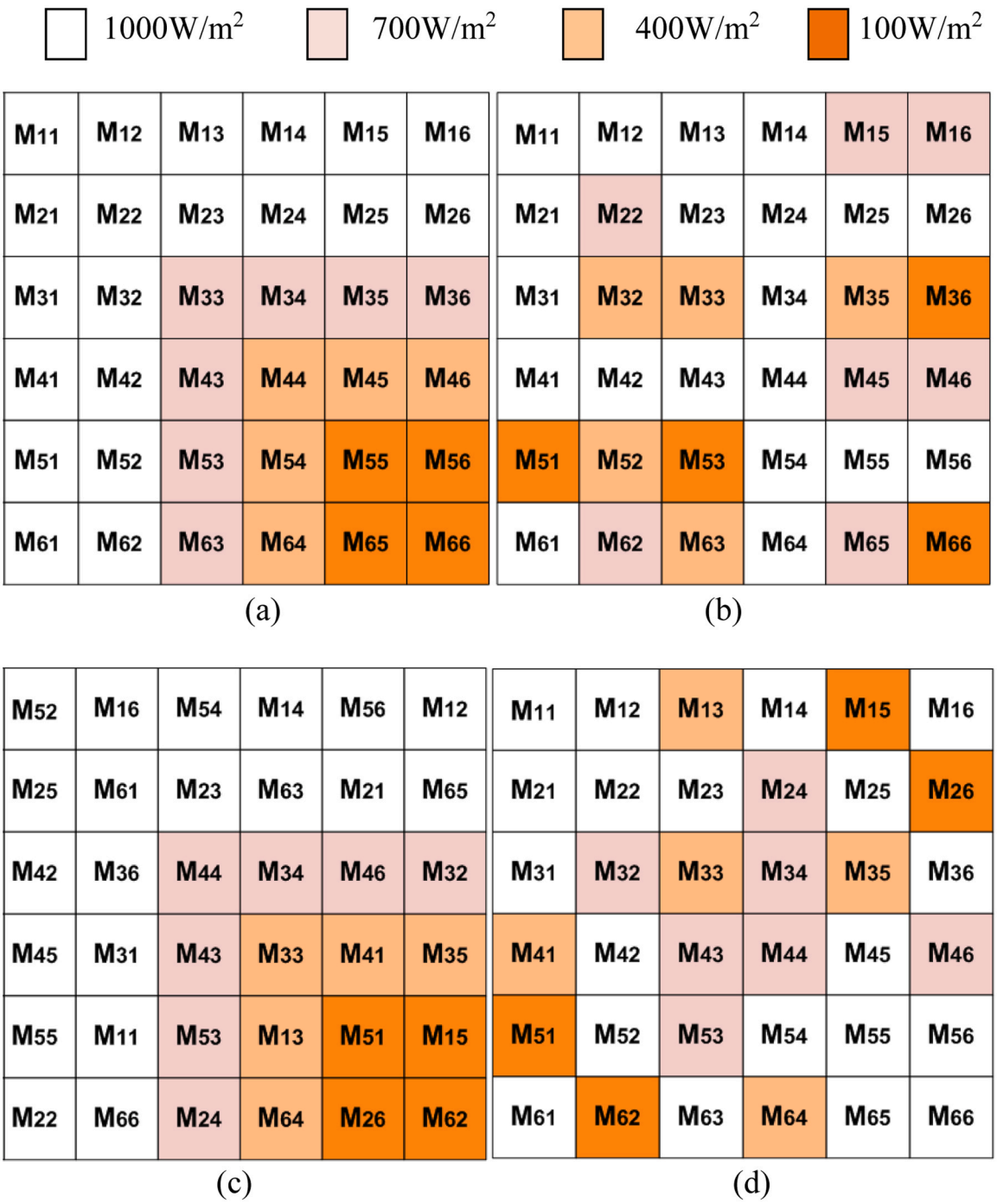

Fig. 10. (a-d): (a) TB shading situation for TCT arrangement, (b) TB shade distribution for ODD-EVEN, (a) TB shading situation for CROSS-KIT configuration, and (b) TB shade dispersion for CROSS-KIT configuration.

6.1. Shading state I

Dwarf Broad is the name given to the shading design because it shades the majority of the columns but very few rows. Knowing the current produced from every row of the PV array is necessary in order to locate global maxima. For various irradiance levels, the row current of modules is calculated as Eq. (9):

Table 4
Spot of Global Peak in TCT, OE and CROSS-KIT assemblies-Shading state-II.

TCT arrangement				**Odd-Even arrangement**				**Cross-Kit arrangement**			
Row current with panels bypassed in the specified sequence		Voltage (V_a)	Power (P_a)	Row current with panels bypassed in the specified sequence		Voltage (V_a)	Power (P_a)	Row current with panels bypassed in the specified sequence		Voltage (V_a)	Power (P_a)
I_{R6}	3.3 I_m	6 V_m	19.8 V_m I_m	I_{R3}	3.3 I_m	6 V_m	19.8 V_m I_m	I_{R3}	4.2 I_m	6 V_m	25.2 V_m I_m
I_{R5}	3.3 I_m	-	-	I_{R5}	3.6 I_m	5 V_m	18.0 V_m I_m	I_{R6}	4.5 I_m	5 V_m	22.5 V_m I_m
I_{R4}	3.9 I_m	4 V_m	15.6 V_m I_m	I_{R6}	3.9 I_m	4 V_m	15.6 V_m I_m	I_{R4}	4.5 I_m	-	18.0 V_m I_m
I_{R3}	4.8 I_m	3 V_m	14.4 V_m I_m	I_{R4}	5.4 I_m	3 V_m	16.2 V_m I_m	I_{R1}	4.5 I_m	-	13.5 V_m I_m
I_{R2}	6.0 I_m	2 V_m	12.0 V_m I_m	I_{R1}	5.4 I_m	-	-	I_{R5}	4.8 I_m	2 V_m	9.2 V_m I_m
I_{R1}	6.0 I_m	-	-	I_{R2}	5.7 I_m	1 V_m	5.7 V_m I_m	I_{R2}	4.8 I_m	-	4.8 V_m I_m

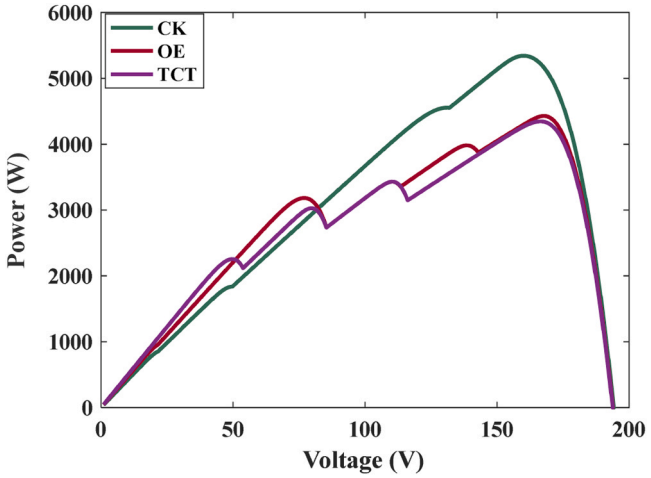

(a). P-V curve Shading state II.

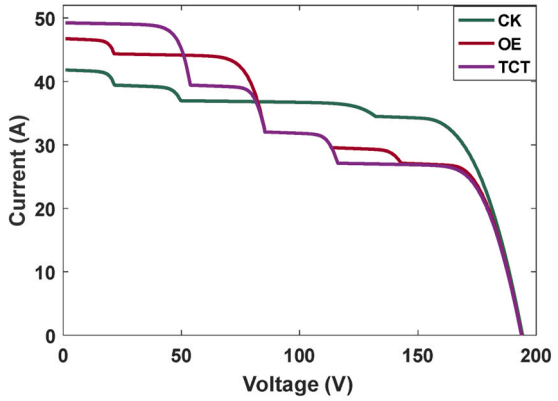

(b). I-V curve Shading state II.

Fig. 11. (a). P-V curve Shading state II. (b). I-V curve Shading state II.

$$I_i = \sum_{j=n}^{i} K_n S_n I_m \tag{9}$$

where n is a range of irradiance conditions, K_n is the number of modules experiencing each irradiance condition, S_n is the shade percentage at each condition, and I_m is the module current during normal operating conditions. The PV array configurations for this situation in Fig. 8(a-d) are TCT, ODD-EVEN, and CROSS-KIT, respectively. It delivers module voltage and current in accordance with the sequence in which the modules are bypassed. The P-V and I-V characteristics of the TCT setup array are referred in Figs. 9(a) and 9 (b). Table 3 shows that three of the six rows have different current values, which cause multiple maxima in the P-V curve, as revealed in Fig. 9(a) for TCT and ODD-EVEN. The PV array's maximum power output is 3993 W in a TCT arrangement and 4372 W in an ODD-

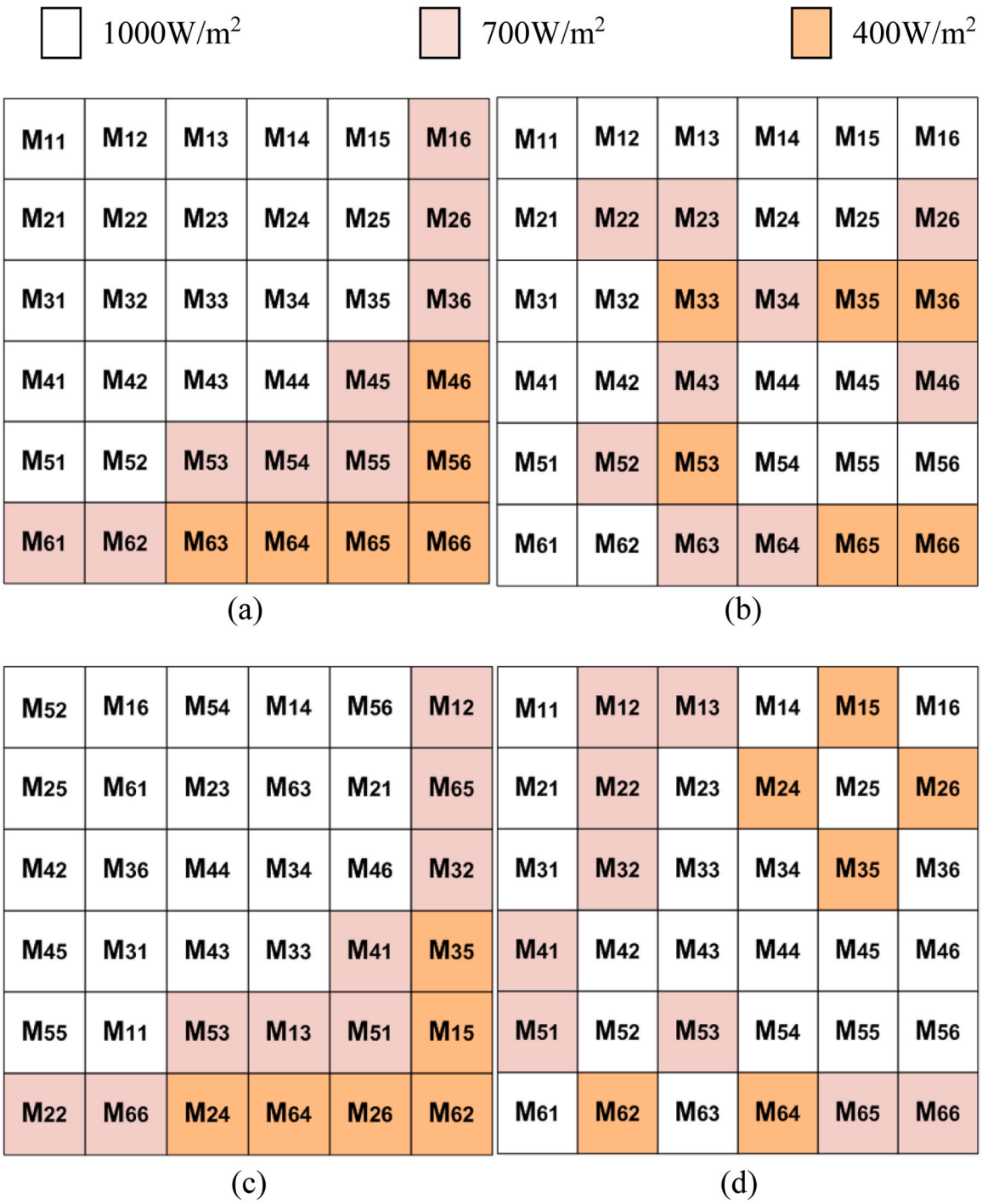

Fig. 12. (a-d): (a) DN shading situation for TCT arrangement, (b) DN shade distribution for ODD-EVEN, (a) DN shading situation for CROSS-KIT configuration, and (b) DN shade dispersion for CROSS-KIT configuration.

EVEN arrangement. Nevertheless, the global maximum (GM) location shifts toward the PV array's standard voltage after the modules were reconfigured according to the CROSS-KIT structure. Additionally, the power produced by the PV array has improved to 5450 W for CROSS-KIT.

Table 5
Spot of Global Peak in TCT, OE and CROSS-KIT assemblies-Shading state III.

TCT arrangement				Odd-Even arrangement				Cross-Kit arrangement			
Row current with panels bypassed in the specified sequence		Voltage (V_a)	Power (P_a)	Row current with panels bypassed in the specified sequence		Voltage (V_a)	Power (P_a)	Row current with panels bypassed in the specified sequence		Voltage (V_a)	Power (P_a)
I_{R6}	3.6 I_m	6 V_m	21.6 V_m I_m	I_{R6}	3.6 I_m	6 V_m	21.8 V_m I_m	I_{R6}	4.2 I_m	6 V_m	25.2 V_m I_m
I_{R5}	3.9 I_m	5 V_m	19.5 V_m I_m	I_{R3}	3.9 I_m	5 V_m	19.5 V_m I_m	I_{R1}	4.5 I_m	5 V_m	22.5 V_m I_m
I_{R4}	5.1 I_m	4 V_m	20.4 V_m I_m	I_{R5}	4.1 I_m	4 V_m	16.4 V_m I_m	I_{R5}	4.8 I_m	4 V_m	19.2 V_m I_m
I_{R3}	5.4 I_m	3 V_m	16.2 V_m I_m	I_{R2}	5.1 I_m	3 V_m	15.3 V_m I_m	I_{R2}	4.8 I_m	-	-
I_{R2}	5.4 I_m	-	-	I_{R4}	5.4 I_m	2 V_m	10.8 V_m I_m	I_{R3}	5.1 I_m	2 V_m	10.2 V_m I_m
I_{R1}	5.4 I_m	-	-	I_{R1}	6.0 I_m	1 V_m	6.0 V_m I_m	I_{R4}	4.4 I_m	1 V_m	5.4 V_m I_m

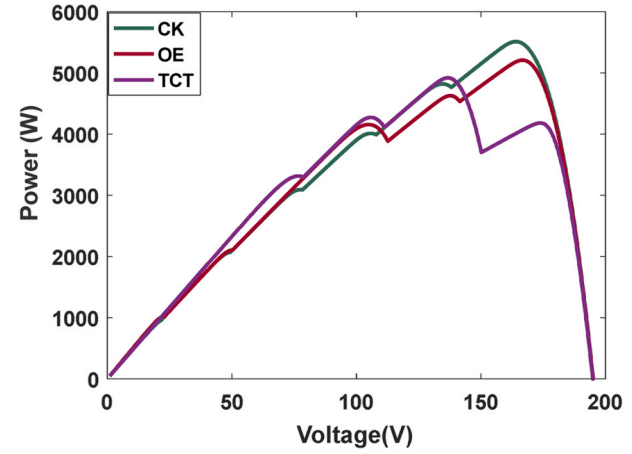

(a). P-V curve Shading state III.

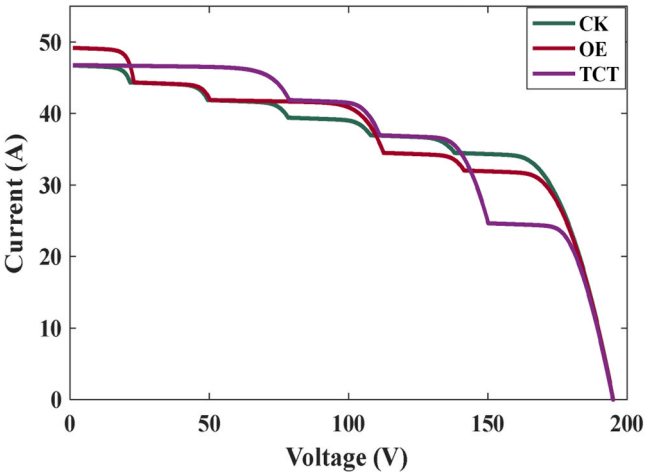

(b). I-V curve Shading state III.

Fig. 13. (a). P-V curve Shading state III. (b). I-V curve Shading state III.

6.2. Shading state II

Based on the tall-broad shading arrangement shown in Fig. 10(a-d), the PV array is alienated into three distinct bands. For a tall-broad shading arrangement, Table 4 mathematically compares a PV array with a TCT configuration, an ODD-EVEN reconfiguration, and one with a CROSS-KIT reconfiguration. Row currents, voltages and peak powers are calculated for this shading situation. The CK design, row 3, is bypassed to maximise the PV array's power output. Figs. 11(a) and 11(b) present an array's P-V and I-V characteristics. The proposed structure's PV array can produce 5343 W of power at its peak. The global peak occurs at 160 V, but before module redesign, the maximum power in the TCT arrangement was 4346 W, and in the ODD-EVEN arrangement was 4429 W. Hence,

Table 6
Spot of Global Peak in TCT, OE, and CROSS-KIT assemblies, Shading state IV.

TCT arrangement				**Odd-Even arrangement**				**Cross-Kit arrangement**			
Row current with panels bypassed in the specified sequence		Voltage (V_a)	Power (P_a)	Row current with panels bypassed in the specified sequence		Voltage (V_a)	Power (P_a)	Row current with panels bypassed in the specified sequence		Voltage (V_a)	Power (P_a)
I_{R6}	2.4 I_m	6 V_m	14.4 V_m I_m	I_{R3}	3.0 I_m	6 V_m	18.0 V_m I_m	I_{R6}	3.9 I_m	6 V_m	23.4 V_m I_m
I_{R5}	3.3 I_m	5 V_m	16.5 V_m I_m	I_{R6}	3.6 I_m	5 V_m	18.0 V_m I_m	I_{R2}	3.9 I_m	-	-
I_{R4}	4.2 I_m	4 V_m	16.8 V_m I_m	I_{R5}	3.9 I_m	4 V_m	15.6 V_m I_m	I_{R1}	3.9 I_m	-	-
I_{R3}	4.8 I_m	3 V_m	14.4 V_m I_m	I_{R2}	4.8 I_m	3 V_m	14.4 V_m I_m	I_{R3}	4.2 I_m	3 V_m	12.6 V_m I_m
I_{R2}	5.4 I_m	2 V_m	10.8 V_m I_m	I_{R4}	5.1 I_m	2 V_m	10.2 V_m I_m	I_{R4}	4.8 I_m	2 V_m	9.6 V_m I_m
I_{R1}	5.4 I_m	-	-	I_{R1}	5.1 I_m	-	-	I_{R5}	5.1 I_m	1 V_m	5.1 V_m I_m

the generated power has increased by 18.65% for the TCT arrangement and by 17.10% for the ODD-EVEN arrangement.

6.3. Shading state III

The dwarf narrow mismatch arrangement is evaluated on TCT configurations with CK structures, as shown in Fig. 12(a-d). Table 5 compares the PV array mathematically with a TCT configuration, an ODD-EVEN reconfiguration, and a CROSS-KIT arrangement. While Figs. 13(a) and 13(b) present its P-V and I-V curves. The P-V curve confirms that the optimum power for the CROSS-KIT arrangement is increased to 5511 W from 4919 W for the TCT arrangement and to 5511 W from 5208 W for the ODD-EVEN arrangement. That is 10.74% and 5.49% more power than the TCT and ODD-EVEN reconfiguration, respectively.

6.4. Shading state IV

Under the same irradiance levels, Table 6 presents the PV array's row current, voltage, and power output. The PV array structure for this situation is shown in Fig. 14(a-d) for TCT, ODD-EVEN, and CROSS-KIT, respectively. While Figs. 15(a) and 15(b) present their P-V and I-V characteristics. These outcomes indicate that the optimum peaks of the TCT, ODD-EVEN and CROSS-KIT structures occur at the standard voltage of the PV array. However, the optimum power produced by the proposed design is enhanced to 4842 W from 3699 W for the TCT arrangement and to 4842 W from 4059 W for the ODD-EVEN arrangement. That is 23.60% and 16.17% more power than the TCT and CROSS-KIT configuration, respectively.

7. Comparative evaluation

The suggested CROSS-KIT approach boosts the PV array's capacity to harvest maximum power in comparison with TCT and OE technique. Table 7 shows that for all four shading states, the maximum power production of the PV array is enhanced with the suggested CROSS-KIT approach. According to Table 8, the proposed CROSS-KIT technique's power enhancement percentage ranges from 5.49% to 26.73%. The comparative Power-Voltage characteristics, as presented in Figs. 9(a), 11(a), 13 (a) & 15(a), clearly show the number of dominant peaks is reduced to 1–2 with the proposed CK algorithm. Whereas with other techniques, the number of peaks is much higher. The complexity of the MPPT algorithm depends on the number of maxima in the Power-Voltage characteristics. As the number of peaks is reduced, comparatively less complex MPPT algorithms can be designed along with the PV array reconfiguration.

7.1. Shading loss

Shading and mismatch losses comprise the two categories of power losses brought on by partial shade. The shading losses result from a reduction in insolation brought on by nearby developments' shading, passing clouds, etc. Consequently, it is challenging to prevent these shading losses. The peak power output of a PV array under standard insolation and the addition of the peak power output of individual panels in a PV array operating in partial shading conditions are represented by shading losses. The shading losses are given in Eq. (10).

$$P_{SL} = P_{max,s} - P_{max,r} \tag{10}$$

With the help of Eq. (10), shading losses are estimated and displayed in Table 9 for various array configurations. Fig. 16 provides a visual representation of the comparison. The shading losses are unavoidable in all practical operating conditions. The shading losses indicate the extent of the shade. For all configurations, the maximum power is the same under normal insolation. The peak power output of a PV array's individual panels' algebraic sums is also constant across all configurations for a given shading environment. As a result, for a specific shading state, shading losses are the same, resulting in identical bars in Fig. 16.

7.2. Mismatch losses

The mismatch losses occur due to differences in irradiance level on panels operating in a PV array. The mismatch losses are calculated as the difference between a PV array's total peak output and the sum of each panel's maximum power [30]. Eq. (11)

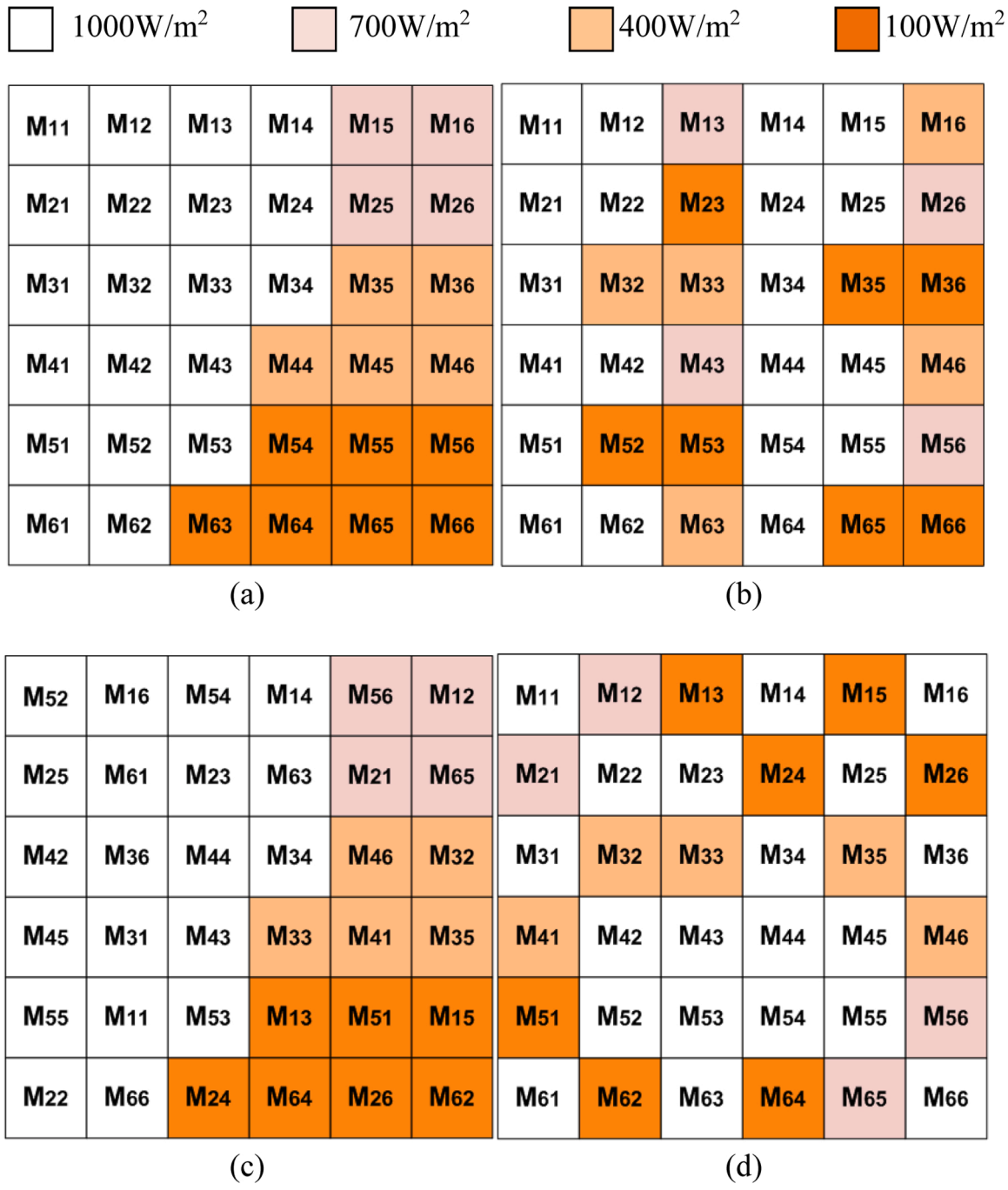

Fig. 14. (a-d): (a) TN shading situation for TCT arrangement, (b) TN shade distribution for ODD-EVEN, (a) TN shading situation for CROSS-KIT configuration, and (b) TN shade dispersion for CROSS-KIT configuration.

calculates mismatch losses.

$$P_{ML} = P_{max,r} - P_{amp} \tag{11}$$

P_{ML} provides mismatch losses in Eq. (11). And percentage mismatch losses for the above shading states are presented in Fig. 17. The PV array's absolute maximum power (P_{amp}) may be obtained from Tables 3, 4, 5, and 6. $P_{max,r}$ indicates the total maximum output of each panel under a specific partial shading situation. There are four distinct insolation levels in each of the four shading states that were taken into consideration.

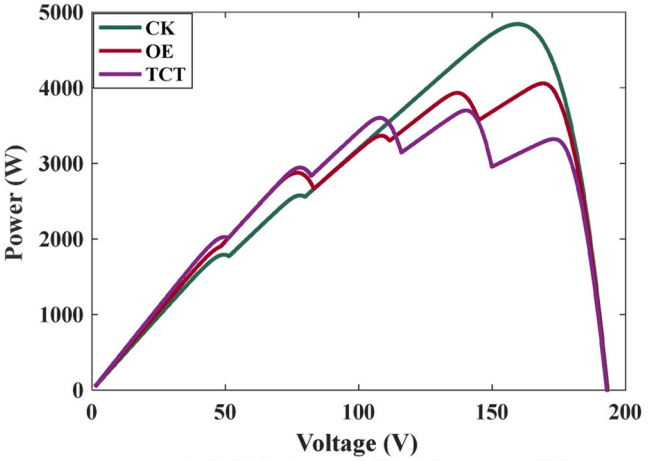

Fig. 15. (a). P-V curve Shading state IV. (b). I-V curve Shading state IV.

Table 7
Comparison of the power produced by the suggested CROSS-KIT approach with TCT and OE techniques.

Shading Situation	TCT (W)	ODD-EVEN (W)	CROSS-KIT (W)
Shading state I	3993	4371	5450
Shading state II	4346	4429	5343
Shading state III	4919	5208	5511
Shading state IV	3699	4059	4842

Table 8
Percentage of power improvement by suggested CROSS-KIT method in comparison with TCT and OE techniques.

Shading Situation	TCT	ODD-EVEN
Shading state I	26.73%	19.79%
Shading state II	18.65%	17.10%
Shading state III	10.74%	05.49%
Shading state IV	23.60%	16.17%

- With an irradiance of 1000 W/m^2 at normal temperature (25 °C), the power production is 200.1 W.
- With an irradiance of 700 W/m^2 at normal temperature (25 °C), the power production is 137.64 W.
- With an irradiance of 400 W/m^2 at normal temperature (25 °C), the power production is 76.89 W.

Table 9
Comparison of shading losses, mismatch losses and percentage execution ratio.

Shading state	Configuration	Shading loss (W)	Mismatch loss (w)	Execution ratio (%)
Shading state I	TCT	1680.84	1529.76	55.43
	ODD-EVEN	1680.84	1151.76	60.67
	CROSS-KIT	1680.84	72.76	75.65
Shading state II	TCT	1740.87	1116.73	60.33
	ODD-EVEN	1740.87	1033.73	61.48
	CROSS-KIT	1740.87	119.73	74.17
Shading state III	TCT	1260.63	1023.97	68.28
	ODD-EVEN	1260.63	734.97	72.29
	CROSS-KIT	1260.63	431.97	76.50
Shading state IV	TCT	2101.05	1403.55	51.34
	ODD-EVEN	2101.05	1043.55	5634
	CROSS-KIT	2101.05	260.55	67.21

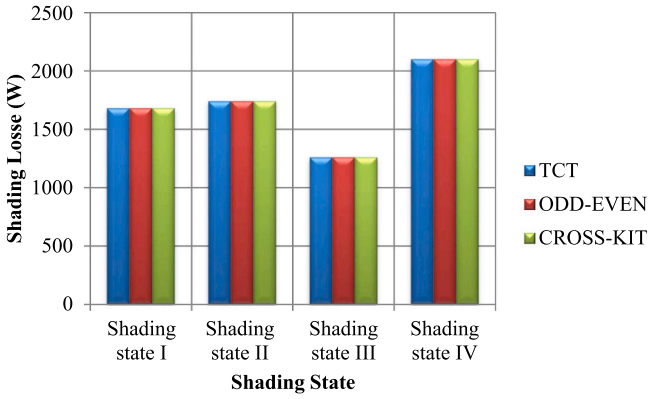

Fig. 16. Shading losses for all considered shading state.

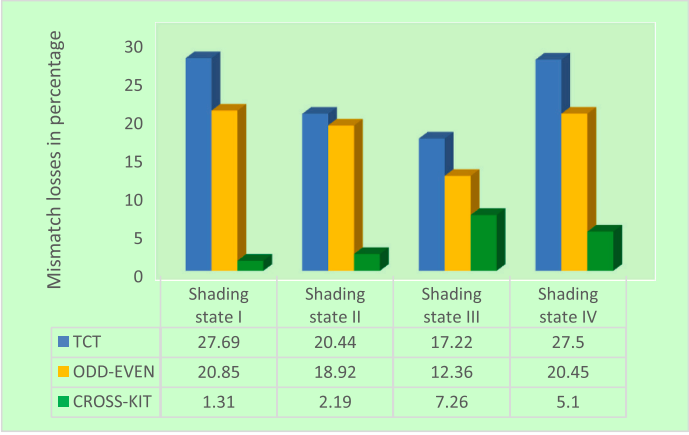

Fig. 17. Mismatch losses in percent for various array configurations.

Table 10
Specification of PV Panel DPJ (1000 W/m^2, 25°C).

Specification	**Values under standard operational circumstances**
Max. power output	10 W
Max. power voltage	25 V
Open circuit voltage	30 V
Max. power current	0.4 A
Short circuit current	0.46 A

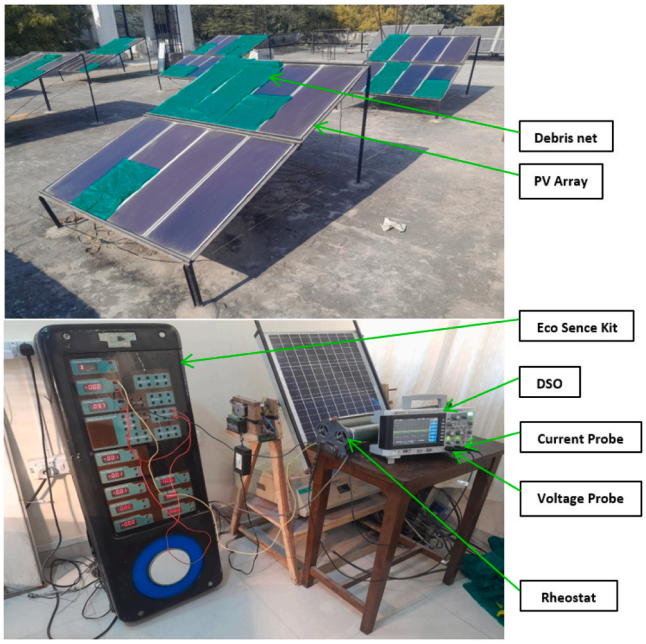

Fig. 18. Experimental for 6 × 6 PV array.

Table 11
Percentage of power improvement by the suggested CROSS-KIT method in comparison with conventional methodology.

Shading Situation	TCT	ODD-EVEN
Shading state I	27.00%	19.72%
Shading state II	19.23%	17.15%
Shading state III	10.98%	06.27%
Shading state IV	23.50%	17.51%

- With an irradiance of 100 W/m^2 at normal temperature (25 °C), the power production is 18.13 W.

The main performance criterion for PV array configurations subject to PSCs is mismatch losses. Row current equalization involves distributing the shade effect on PV array topologies under PSCs. Additionally, decreases in mismatch losses show that a PV array is well structured. It is evident from Table 9 that the proposed CROSS-KIT configuration for all shading states effectively reduces mismatch losses. With the suggested approach, mismatch losses lie in the range of 72.76 W to 431. 97 W. Whereas for ODD-EVEN and TCT, the mismatch losses range from 734.97 W to 1529.76 W.

7.3. Execution ratio

It is defined as the ratio of maximum power output at the partial shading condition and peak power output at standard insolation for the PV array.

The reconfiguration of a PV array in partial shading depends significantly on the execution ratio. Deciding how many shaded modules will be bypassed or disconnected can minimize power loss and increase energy harvesting. Mismatch effects between modules can be reduced by altering the execution ratio, resulting in optimal system performance. Additionally, it increases the lifespan of the array and shields it from potential harm, such as hotspots. The PV array can run effectively, maximizing overall performance and energy production with the proper execution ratio. It is evident from Table 9 that the proposed CROSS-KIT configuration for all shading states have higher execution ratio in comparison with ODD-EVEN and TCT.

8. Experimental validation

The suggested CROSS-KIT approach is used to design a PV array, and their results were compared with the ODD-EVEN and TCT methods. Table 10 lists the specification of the PV module that are being considered. A PV array of 6 × 6 (36 modules) order is used for the investigational examination, as illustrated in Fig. 17.

The debris nets offer non-uniform irradiance or partial shade to PV arrays. The sun's irradiance over each PV module is controlled

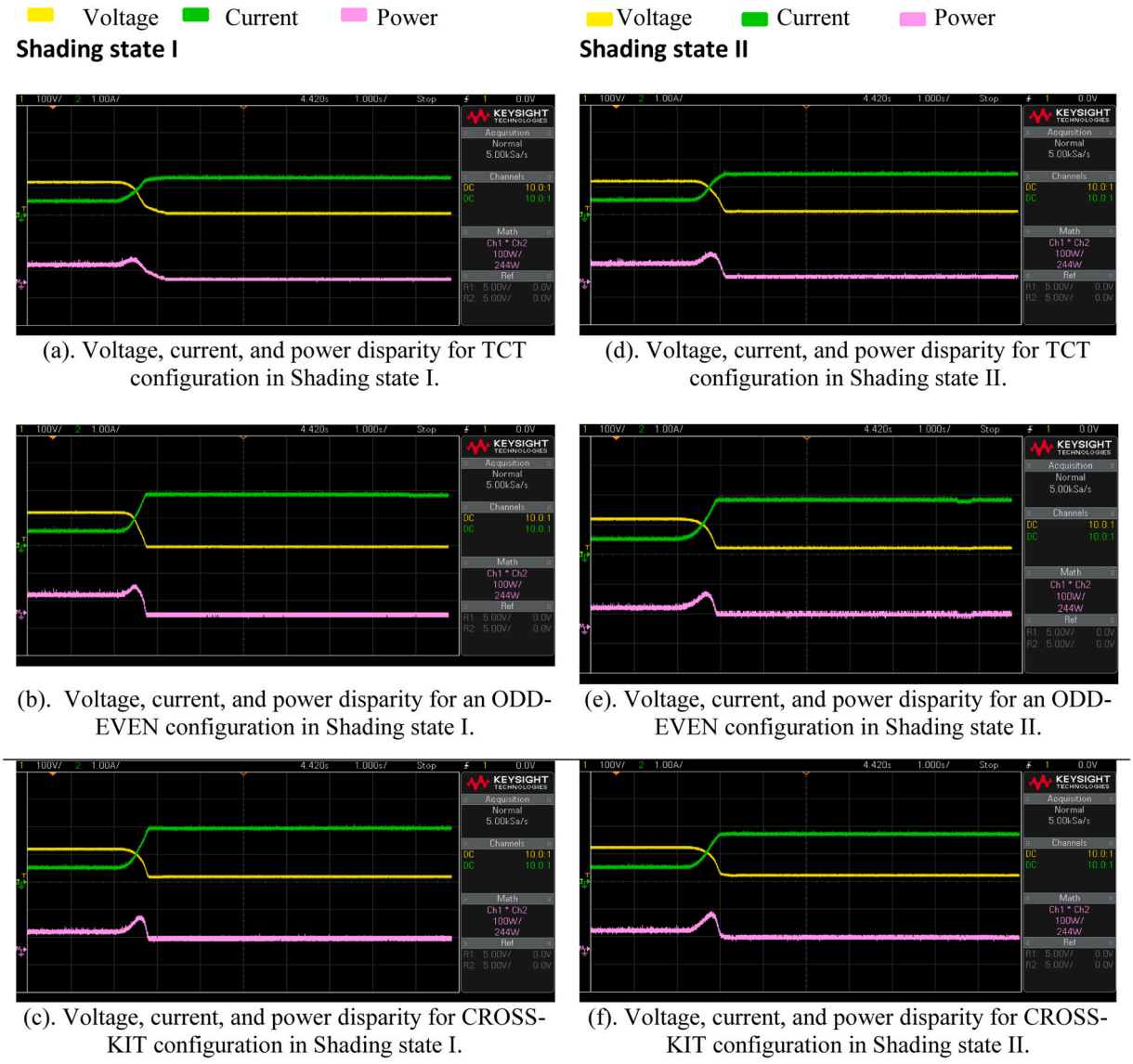

Fig. 19. (a–l). Voltage, current, and power characteristics of an experimental setup (a-c) for Shading state I, (d-f) for Shading state II, (g-i) for Shading state III, and (j-l) for Shading state IV.

with the help of measurements of the size and number of layers of debris net on each PV module. Therefore, any partial shade situation for a PV array can be implemented. All of the shading cases shown in Figs. 8, 10, 12, and 14 were considered for the comparative study. The PV array is coupled to the changeable resistive load. The current probe and voltage probe give the input to the Digital Storage Oscilloscope (DSO, 50 MHz, 1 GSa/s). The current and voltage levels at a given moment is available at DSO, and also shows the variation of power in accordance with these current and voltage. For shading states, I, II, III, and IV, respectively, Fig. 18 displays the characteristics of the current voltage and power. These statistics clearly show that the suggested CROSS-KIT approach significantly increases the array's power output, as shown in Table 11, while closely resembling the features presented in the simulation outcomes. Fig. 19.

9. Conclusion

The CROSS-KIT approach is presented in this study for PV arrays that are permanent structures of PV modules. The outcomes indicate an increase in the PV array's power generation under PSC circumstances. The location of the optimum power point demonstrates that the row currents are bypassed to get the highest possible power output. When the modules in a TCT-designed array have bypass diodes connected antiparallel, the array's optimum output power rises. But it results in several crests in P-V plots. The

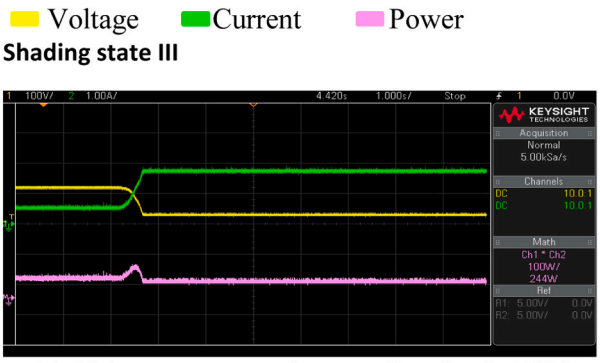

(g). Voltage, current, and power disparity for TCT configuration in Shading state III.

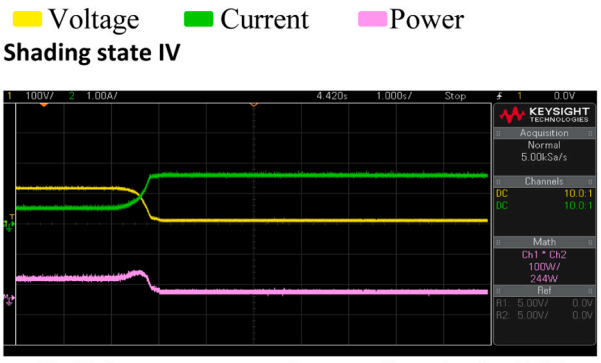

(j). Voltage, current, and power disparity for TCT configuration in Shading state IV.

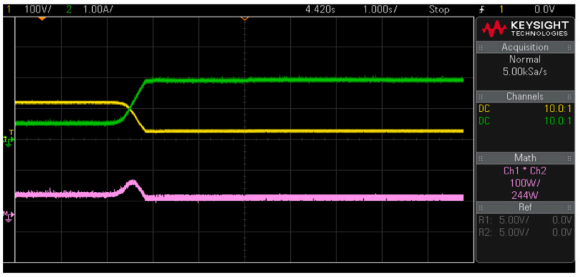

(h). Voltage, current, and power disparity for an ODD-EVEN configuration in Shading state III.

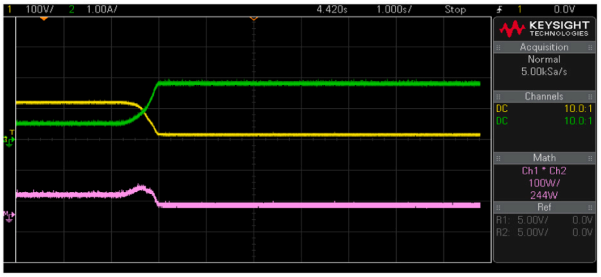

(k). Voltage, current, and power disparity for an ODD-EVEN configuration in Shading state III.

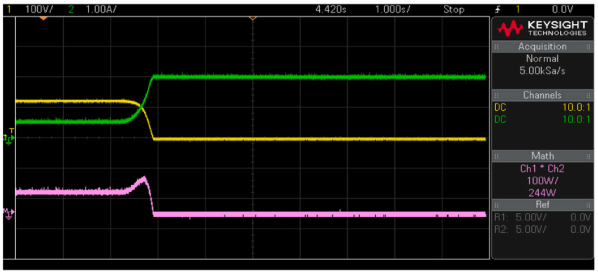

(i). Voltage, current, and power disparity for the CROSS-KIT configuration in Shading state IV.

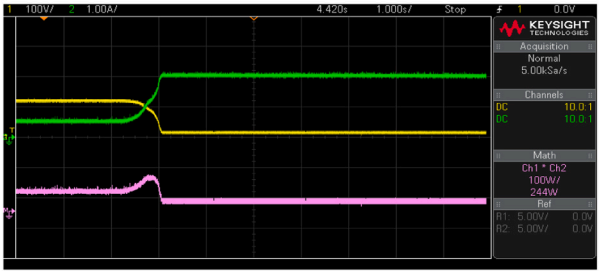

(l). Voltage, current, and power disparity for the CROSS-KIT configuration in Shading state IV.

Fig. 19. (*continued*).

traditional MPPT method will be insufficient. The suggested method simplifies MPPT by reducing numerous peaks. The following are specific outcomes of the PV array reconfigured with the CROSS-KIT technique:

- There is an increase in output power in the planned CROSS-KIT arrangement of 26.73% in comparison to the output power offered by the TCT arrangement and 19.79% in comparison to the output power caused by the ODD-EVEN arrangement for the dwarf broad shading configured structure.
- The highest power production for a CROSS-KIT configuration for a tall-broad shading situation is 5343 W, compared to 4346 W for a TCT arrangement and 4429 W for an ODD-EVEN arrangement, respectively.
- For Shading state III, the maximum power outputs of the TCT configured structure, the CROSS-KIT configured structure, and the CROSS-KIT structure are 4919 W, 5208 W, and 5511 W, respectively.
- Maximum power output for the tall narrow shading scheme is 4842 W for a CROSS-KIT structure, 4059 W for an ODD-EVEN structure, and 3699 W for a TCT setup.
- The proposed structure of the PV array boosts power production, as shown in Table 9 and decreases several local maxima for various shading conditions.

Declaration of Competing Interest

The authors declare that they have no known competing financial interests or personal relationships that could have appeared to influence the work reported in this paper.

Data availability

Data will be made available on request.

References

[1] T. Adefarati, R.C. Bansal, Integration of renewable distributed generators into the distribution system: a review, IET Renew. Power Gener. 10 (7) (2016) 873–884, https://doi.org/10.1049/iet-rpg.2015.0378.

[2] K. Nghitevelekwa, R.C. Bansal, A review of generation dispatch with large-scale photovoltaic systems, Renew. Sustain. Energy Rev. 81 (2018) (2018) 615–624, https://doi.org/10.1016/j.rser.2017.08.035.

[3] R. Dubey, D. Joshi, R.C. Bansal, Optimization of solar photovoltaic plant and economic analysis, Electr. Power Compon. Syst. 44 (18) (2016) 2025–2035, https://doi.org/10.1080/15325008.2016.1209706.

[4] S. Khatoon, Ibraheem, and M.F. Jalil, Analysis of solar photovoltaic array under partial shading conditions for different array configurations, in Innovative Applications of Computational Intelligence on Power, Energy and Controls with their impact on Humanity (CIPECH), IEEE, Nov. 2014, pp. 452–456. doi: 10.1109/CIPECH.2014.7019127.

[5] S. Khatoon, Ibraheem, and M.F. Jalil, Feasibility analysis of solar photovoltaic array configurations under partial shading conditions, in 2015 Annual IEEE India Conference (INDICON), IEEE, Dec. 2015, pp. 1–6. doi: 10.1109/INDICON.2015.7443701.

[6] M.S. Bin Arif, U. Mustafa, S. bin Md Ayob, Extensively used conventional and selected advanced maximum power point tracking techniques for solar photovoltaic applications: An overview, AIMS Energy 8 (5) (2020) 935–958, https://doi.org/10.3934/ENERGY.2020.5.935.

[7] G. Li, Y. Jin, M.W. Akram, X. Chen, J. Ji, Application of bio-inspired algorithms in maximum power point tracking for PV systems under partial shading conditions – A review. Renewable and Sustainable Energy Reviews 81, Elsevier Ltd,, 2018, pp. 840–873, https://doi.org/10.1016/j.rser.2017.08.034.

[8] Y. Jin, W. Hou, G. Li, X. Chen, A glowworm swarm optimization-based maximum power point tracking for photovoltaic/thermal systems under non-uniform solar irradiation and temperature distribution (Apr.), Energies 10 (4) (2017), https://doi.org/10.3390/en10040541.

[9] Y.J. Wang, P.C. Hsu, An investigation on partial shading of PV modules with different connection configurations of PV cells, Energy 36 (5) (2011) 3069–3078, https://doi.org/10.1016/j.energy.2011.02.052.

[10] S.R. Pendem, S. Mikkili, Modeling, simulation and performance analysis of solar PV array configurations (Series, Series–Parallel and Honey-Comb) to extract maximum power under Partial Shading Conditions, Energy Rep. 4 (2018) 274–287, https://doi.org/10.1016/j.egyr.2018.03.003.

[11] N.D. Kaushika, N.K. Gautam, Energy yield simulations of interconnected solar PV arrays, IEEE Trans. Energy Convers. 18 (1) (2003) 127–134, https://doi.org/10.1109/TEC.2002.805204.

[12] D. Sharma, M.F. Jalil, M.S. Ansari, R.C. Bansal, A review of PV array reconfiguration techniques for maximum power extraction under partial shading conditions, Optik (2023), 170559, https://doi.org/10.1016/j.ijleo.2023.170559.

[13] M.F. Jalil, S. Khatoon, I. Nasiruddin, R.C. Bansal, An improved feasibility analysis of photovoltaic array configurations and reconfiguration under partial shading conditions, Electr. Power Compon. Syst. 48 (9–10) (2020) 1077–1089, https://doi.org/10.1080/15325008.2020.1821842.

[14] S. Kabir, R. Bansal, and M. Nadarajah, Effects of partial shading on Photovoltaic with advanced MPPT scheme, in PECon- IEEE International Conference on Power and Energy, 2012, pp. 354–359. doi: 10.1109/PECon.2012.6450237.

[15] A. Laudani, G.M. Lozito, V. Lucaferri, M. Radicioni, and F.R. Fulginei, On circuital topologies and reconfiguration strategies for PV systems in partial shading conditions: A review, AIMS Energy, vol. 6, no. 5. AIMS Press, pp. 735–763, 2018. doi: 10.3934/energy.2018.5.735.

[16] M.F.N. Tajuddin, M.S. Arif, S.M. Ayob, Z. Salam, Perturbative methods for maximum power point tracking (MPPT) of photovoltaic (PV) systems: A review, Int. J. Energy Res. 39 (9) (2015) 1153–1178, https://doi.org/10.1002/er.3289. John Wiley and Sons Ltd.

[17] D. la Manna, V. Li Vigni, E. Riva Sanseverino, V. di Dio, P. Romano, Reconfigurable electrical interconnection strategies for photovoltaic arrays: A review. Renewable and Sustainable Energy Reviews 33, Elsevier Ltd,, 2014, pp. 412–426, https://doi.org/10.1016/j.rser.2014.01.070.

[18] G. Spagnuolo, G. Petrone, B. Lehman, C.A. Ramos Paja, Y. Zhao, M.L. Orozco Gutierrez, Control of photovoltaic arrays: Dynamical reconfiguration for fighting mismatched conditions and meeting load requests, IEEE Ind. Electron. Mag. 9 (1) (2015) 62–76, https://doi.org/10.1109/MIE.2014.2360721.

[19] B.I. Rani, G.S. Ilango, C. Nagamani, Enhanced power generation from PV array under partial shading conditions by shade dispersion using Su Do Ku configuration, IEEE Trans. Sustain Energy 4 (3) (2013) 594–601, https://doi.org/10.1109/TSTE.2012.2230033.

[20] M. Horoufiany, R. Ghandehari, Optimization of the Sudoku based reconfiguration technique for PV arrays power enhancement under mutual shading conditions, Sol. Energy 159 (2018) 1037–1046, https://doi.org/10.1016/j.solener.2017.05.059.

[21] B. Dhanalakshmi, N. Rajasekar, Dominance square based array reconfiguration scheme for power loss reduction in solar Photovoltaic (PV) systems, Energy Convers. Manag 156 (October 2017) (2018) 84–102, https://doi.org/10.1016/j.enconman.2017.10.080.

[22] P.R. Satpathy, R. Sharma, Power loss reduction in partially shaded PV arrays by a static SDP technique, Energy 156 (2018) 569–585, https://doi.org/10.1016/j.energy.2018.05.131.

[23] M.S.S. Nihanth, J.P. Ram, D.S. Pillai, A.M.Y.M. Ghias, A. Garg, N. Rajasekar, Enhanced power production in PV arrays using a new skyscraper puzzle based one-time reconfiguration procedure under partial shade conditions (PSCs, Sol. Energy 194 (May) (2019) 209–224, https://doi.org/10.1016/j.solener.2019.10.020.

[24] A. Calcabrini, M. Muttillo, R. Weegink, P. Manganiello, M. Zeman, O. Isabella, A fully reconfigurable series-parallel photovoltaic module for higher energy yields in urban environments, Renew. Energy 179 (2021) 1–11, https://doi.org/10.1016/j.renene.2021.07.010.

[25] G. Sai Krishna, T. Moger, A novel adaptive dynamic photovoltaic reconfiguration system to mitigate mismatch effects, Renew. Sustain. Energy Rev. 141 (2021), https://doi.org/10.1016/j.rser.2021.110754.

[26] D. Nguyen, B. Lehman, An adaptive solar photovoltaic array using model-based reconfiguration algorithm, IEEE Trans. Ind. Electron. 55 (7) (2008) 2644–2654, https://doi.org/10.1109/TIE.2008.924169.

[27] G. Velasco-Quesada, F. Guinjoan-Gispert, R. Pique-Lopez, M. Roman-Lumbreras, A. Conesa-Roca, Electrical PV array reconfiguration strategy for energy extraction improvement in grid-connected PV Systems, IEEE Trans. Ind. Electron. 56 (11) (2009) 4319–4331, https://doi.org/10.1109/TIE.2009.2024664.

[28] D. Yousri, S.B. Thanikanti, K. Balasubramanian, A. Osama, A. Fathy, Multi-objective grey wolf optimizer for optimal design of switching matrix for shaded PV array dynamic reconfiguration, IEEE Access 8 (2020) 159931–159946, https://doi.org/10.1109/ACCESS.2020.3018722.

[29] M.Z. Shams El-Dein, M. Kazerani, M.M.A. Salama, Optimal photovoltaic array reconfiguration to reduce partial shading losses, IEEE Trans. Sustain Energy 4 (1) (2013) 145–153, https://doi.org/10.1109/TSTE.2012.2208128.

[30] J.P. Storey, P.R. Wilson, D. Bagnall, Improved optimization strategy for irradiance equalization in dynamic photovoltaic arrays, IEEE Trans. Power Electron 28 (6) (2013) 2946–2956, https://doi.org/10.1109/TPEL.2012.2221481.

[31] B. Yang, et al., PV Arrays Reconfiguration for Partial Shading Mitigation: Recent Advances, Challenges and Perspectives, Energy Conversion and Management, Elsevier Ltd,, 2021, https://doi.org/10.1016/j.enconman.2021.114738.

[32] M. Akrami, K. Pourhossein, A novel reconfiguration procedure to extract maximum power from partially-shaded photovoltaic arrays, Sol. Energy 173 (December 2017) (2018) 110–119, https://doi.org/10.1016/j.solener.2018.06.067.

[33] Z. Zhu, M. Hou, L. Ding, G. Zhu, Z. Jin, Optimal photovoltaic array dynamic reconfiguration strategy based on direct power evaluation, IEEE Access 8 (2020) 210267–210276, https://doi.org/10.1109/ACCESS.2020.3036124.
[34] S. Khatoon, M.F. Jalil, R. Aman, Modeling and performance analysis of a PV system under mismatch scenarios. Lecture Notes in Electrical Engineering, Springer Science and Business Media Deutschland GmbH,, 2022, pp. 387–395, https://doi.org/10.1007/978-981-16-7472-3_31.
[35] A. Tabanjat, M. Becherif, D. Hissel, Reconfiguration solution for shaded PV panels using switching control, Renew. Energy 82 (2015) 4–13, https://doi.org/10.1016/j.renene.2014.09.041.
[36] K.Ş. Parlak, PV array reconfiguration method under partial shading conditions, Int. J. Electr. Power Energy Syst. 63 (2014) 713–721, https://doi.org/10.1016/j.ijepes.2014.06.042.
[37] M.Z. Shams El-Dein, M. Kazerani, M.M.A. Salama, An optimal total cross tied interconnection for reducing mismatch losses in photovoltaic arrays, IEEE Trans. Sustain Energy 4 (1) (2013) 99–107, https://doi.org/10.1109/TSTE.2012.2202325.
[38] P. Srinivasa Rao, G. Saravana Ilango, C. Nagamani, Maximum power from PV arrays using a fixed configuration under different shading conditions, IEEE J. Photo 4 (2) (2014) 679–686, https://doi.org/10.1109/JPHOTOV.2014.2300239.
[39] I. Nasiruddin, S. Khatoon, M.F. Jalil, R.C. Bansal, Shade diffusion of partial shaded PV array by using odd-even structure, Sol. Energy 181 (2019) 519–529, https://doi.org/10.1016/j.solener.2019.01.076.
[40] M.G. Villalva, J.R. Gazoli, E.R. Filho, Comprehensive approach to modeling and simulation of photovoltaic arrays, IEEE Trans. Power Electron 24 (5) (2009) 1198–1208, https://doi.org/10.1109/TPEL.2009.2013862.
[41] M.F. Jalil, S. Khatoon, I. Nasiruddin, R.C. Bansal, Review of PV array modelling, configuration and MPPT techniques, Int. J. Model. Simul. 42 (4) (2022) 533–550, https://doi.org/10.1080/02286203.2021.1938810.
[42] M.F. Jalil, S. Ansari, Mohammad Shariz Diwania, M.A. Husain, Performance analysis of PV array connection schemes under mismatch scenarios, in: A. Iqbal, H. Malik, A. Riyaz, K. Abdellah, S. Bayhan (Eds.), Lecture Notes in Electrical Engineering 723, Springer Singapore, Singapore, 2021, pp. 225–235, https://doi.org/10.1007/978-981-33-4080-0.
[43] M.A. Husain, M.F. Jalil, M.T.S. Beg, M. Naseem, A. Tariq, Modeling and study of a standalone PV system using MATLAB/SIMULINK,", i-manager's J. Electr. Eng. 5 (4) (2012) 30–35, https://doi.org/10.26634/jee.5.4.1863.